Water level, vegetation composition and plant productivity explain greenhouse gas fluxes in temperate cutover fens after inundation

M. Minke[1/5], J. Augustin[2], A. Burlo[3], T. Yarmashuk[4], H. Chuvashova[3], A. Thiele[5/6], A. Freibauer[1], V. Tikhonov[3], M. Hoffmann[7]

[1]Thünen Institute of Climate–Smart Agriculture, Braunschweig, Germany

[2]Institute for Landscape Biogeochemistry, ZALF e.V., Müncheberg, Germany

[3]Scientific and Practical Centre of the National Academy of Sciences of Belarus for Biological Resources, Minsk, Belarus,

[4]Institute for Nature Management of the National Academy of Sciences of Belarus, Minsk, Belarus

[5]Institute of Botany and Landscape Ecology, University Greifswald, Germany

[6]Michael Succow Foundation, Greifswald, Germany

[7]Institute of Soil Landscape Research, ZALF e.V., Müncheberg, Germany

Abstract

Peat extraction leaves a land surface with a strong relief of deep cutover areas and higher ridges. Rewetting inundates the deep parts while less deeply extracted zones remain at or above the water level. In temperate fens the flooded areas are colonized by helophytes such as *Eriophorum angustifolium*, *Carex* spp., *Typha latifolia* or *Phragmites australis* dependent on water depth. Reeds of *Typha* and *Phragmites* are reported as large sources of methane, but data on net CO_2 uptake are contradictory for *Typha* and rare for *Phragmites*. Here, we analyze the effect of vegetation, water level and nutrient conditions on greenhouse gas (GHG) emissions for representative vegetation types along water level gradients at two rewetted cutover fens (mesotrophic and eutrophic) in Belarus. Greenhouse gas emissions were measured campaign-wise with manual chambers every two to four weeks for two years and interpolated by modelling.

All sites had negligible nitrous oxide exchange rates. Most sites were carbon sinks and small GHG sources. Methane emissions generally increased with net ecosystem CO_2 uptake. Mesotrophic small sedge reeds with water table around the land surface were small GHG sources in the range of 2.3 to 4.2 t CO_2 eq ha^{-1} yr^{-1}. Eutrophic tall sedge - *Typha latifolia* reeds on newly formed floating mats were substantial net GHG emitters

in the range of 25.1 to 39.1 t CO_2 eq ha^{-1} yr. They represent transient vegetation stages. *Phragmites* reeds ranged between -1.7 to 4.2 t CO_2 eq ha^{-1} yr^{-1} with an overall mean GHG emission of 1.3 t CO_2 eq ha^{-1} yr^{-1}. The annual CO_2 balance was best explained by vegetation biomass, which includes the role of vegetation composition and species. Methane emissions were obviously driven by biological activity of vegetation and soil organisms.

Shallow flooding of cutover temperate fens is a suitable measure to arrive at low GHG emissions. *Phragmites australis* establishment should be promoted in deeper flooded areas and will lead to moderate, but variable GHG emissions or even occasional sinks. The risk of large GHG emissions is higher for eutrophic than mesotrophic peatlands. Nevertheless, flooding of eutrophic temperate fens still represents a safe GHG mitigation option because even the hotspot of our study, the floating tall sedge – *Typha latifolia* reeds, did not exceed the typical range of GHG emissions from drained fen grasslands and the spatially dominant *Phragmites australis* reed emitted by far less GHG than drained fens.

1 Introduction

Cutover peatlands represent about ten percent of all drained peatlands outside the tropics with the main share in the Nordic countries and Eastern Europe (Joosten and Clarke, 2002). Since the 1990s restoration of cutaway peatlands was conducted especially in Canada, Finland, Sweden and Ireland. Similar projects in Eastern Europe started later, but already cover vast areas. 42,000 ha of degraded peatlands were restored in Belarus since 2007 and about 80,000 ha since 2010 in the European part of Russia, aiming to decrease GHG emissions from microbial peat oxidation and peat fire incidents (Tanneberger and Wichtmann, 2011; Wetlands International, 2015).

A large proportion of the peatlands that have been rewetted or are available for rewetting in Russia and Belarus are abandoned cutover fens (Minayeva et al., 2009; Tanovitskaya and Kozulin, 2011). Rewetting of such sites creates a mosaic of wet and flooded zones and elevated drier parts, and results in rapid vegetation changes (Kozulin et al., 2010; Thiele et al., 2011). At sites with the water level close to surface species like *Eriophorum angustifolium*, *Carex vesicaria* and *Lythrum salicaria* establish within a

few years, or, under more nutrient rich conditions, *Calamagrostis canescens*, *Lysimachia thyrsiflora*, *Carex elata* and *Salix*. At flooded areas with standing water depths of more than 20 cm mainly *Phragmites australis* emerges, whereas water levels above 30 cm in the medium term only result in the establishment of submerse and floating plants (Kozulin et al., 2010; Thiele et al., 2011).

Studies from rewetted cutover boreal peatlands and temperate bogs show that methane and carbon dioxide emissions are strongly related to water level, vegetation, and meteorological conditions (Tuittila et al., 1999, 2000; Drösler, 2005; Yli-Petäys et al., 2007; Soini et al., 2010; Samaritani et al., 2011; Strack and Zuback, 2013; Wilson et al., 2013; Beyer et al., 2015). For rewetting it is frequently recommended to raise the water level throughout the year to close to the surface and to avoid inundation in order to promote the establishment of peat forming vegetation and to prevent high methane emissions (Drösler et al., 2008; Couwenberg et al., 2008, 2011; Joosten et al., 2012). Such conditions have been proven optimal for bog restoration (Beyer et al., 2015), but their feasibility for fens has been questioned (Koebsch et al., 2013; Zak et al., 2015). In practice, fens are often rewetted by shallow flooding.

So far, complete GHG balances are not available for rewetted temperate cutover fens. Such fens differ from those in the above cited studies in particular by the massive establishment of *Typha* and *Phragmites australis* in shallow water, i.e. of species that are potentially strong pathways of methane (Kim et al., 1998; Brix et al., 2001; Whiting and Chanton, 2001; Kankaala et al., 2004; Hendriks et al., 2007; Chu et al., 2015; Knox et al., 2015; Strachan et al., 2015). Whereas earlier studies indicate that the radiative forcing of such methane emissions may be compensated for by the simultaneous very strong net CO_2 uptake (Brix et al., 2001; Whiting and Chanton, 2001), recent observations described *Typha* dominated wetlands as often only weak CO_2 sinks (Rocha and Goulden, 2008; Chu et al., 2015; Strachan et al., 2015; but cf. Knox et al., 2015). Moreover, submerse and floating plants that are promoted by deep flooding have much higher methane production potential than emergent species (Kankaala et al., 2003; Zak et al., 2015).

This study aims to quantify GHG emissions from inundated temperate cutover fens recolonized by wetland plants. We measured for two years the CO_2, CH_4, and N_2O emissions from *Phragmites australis* communities and other representative vegetation types along water level gradients in a mesotrophic and a eutrophic rewetted cutover fen in Belarus. We hypothesize that

(i) all sites are net CO_2 sinks: peat loss by oxidation has stopped after rewetting. The net CO_2 sink increases with nutrient status, the productivity of the vegetation and peaks under shallow inundation,

(ii) methane emissions increase with the productivity of the vegetation and peak under shallow inundation.

(iii) the net GHG balance is near neutral when water levels are close to surface because CH_4 emissions are balanced by the net CO_2 sink. The net GHG balance turns into a source when sites are continuously flooded because the global warming by CH_4 emissions exceeds the net CO_2 sink.

2 Materials and methods

2.1 Study sites

Greenhouse gas fluxes were measured at two sites in Belarus (Fig. 1) with a temperate continental climate with fully humid conditions and warm summers (Dfb after Köppen, 1936; cf. Kottek et al., 2006). Both sites have been subject to peat extraction, but differ with respect to time since rewetting, water depth, peat characteristics and nutrient status, vegetation, and regional climate.

"Barcianicha" (54.10° N; 26.29° E) is located in central Belarus on an alluvial plain between the rivers Al'šanka and Zahodniaia ("Western") Biarėzina and predominantly fed by groundwater discharge (Maksimenkov et al., 2006). In 1990 about 190 ha of Barcianicha were drained and from 1992 to 1995 peat was extracted by milling over an area of 150 ha to a remaining peat depth of about 80 cm. After abandonment ditches were closed with earth dams and water level was raised on 60% of the area, allowing wetland species like *Phragmites australis*, *Carex rostrata* and *Eriophorum angustifolium* to establish (Maksimenkov et al., 2006). Strong water level amplitudes between summer and winter were stabilized in 2007 by weirs and overflow dams. In 2010 most of the area had water levels at or slightly above the surface throughout the year. Tall reeds, dominated by *Phragmites australis* of up to two metres height, covered the area. Three GHG monitoring sites were installed along a water level gradient, including the small sedge reeds *Eriophorum angustifolium–Carex rostrata* (further indicated as BA *Eriophorum–Carex*) and *Carex rostrata–Equisetum fluviatile* (BA *Carex–Equisetum*) at 15 m distance, and a *Phragmites australis–Carex rostrata* reed (BA *Phragmites–Carex*) at another 30 m distance (Table A1).

The second peatland, “Giel’cykaŭ Kašyl”’ (52.38° N; 25.21° E), forms part of the “Bierastaviec” fen and is situated on the left bank of Jasiel’da river. It belongs to the Ramsar site “Sporaŭski zakaznik” and was drained in 1975 (Kadastrovyj spravochnik, 1979). More than one metre of peat remained after peat extraction and grassland was established. But as the area proved to be unsuited for hay production, the pumping station was turned off in 1985. The area was flooded by the Jasiel’da, which is connected with Giel’cykaŭ Kašyl’ by a 300 m long channel. During the vegetation period the area receives additional water pumped out of an adjacent drained fen. *Phragmites australis* of three metres height dominates the area, which is flooded up to one metre above the surface. A 30–80 m wide swampy zone along the edges is formed by *Typha latifolia*, *T. angustifolia*, and tussocks of *Carex elata* and *C. vesicaria* floating on up to one metre of water. GHG monitoring was performed in the floating tall sedge reeds at two sites: a *Carex elata–Lysimachia thyrsiflora* site (GK *Carex–Lysimachia*), and a *Typha latifolia–Hydrocharis morsus–ranae* site (GK *Typha–Hydrocharis*; Table A1), at three metres distance from each other. The third *Phragmites australis–Lemna trisulca* site (GK *Phragmites–Lemna*) was situated 20 m from the first two sites in the deeper inundated main area, separated from the swampy zone by a flooded ditch.

2.2 Site characteristics

Each site was split into three plots. Peat depth, stratigraphy and degree of decomposition after Von Post (AG Boden, 2005) were determined for each site using a chamber corer (50 cm long, 5 cm diameter). One mixed surface peat sample (0–5 cm) from each plot was analysed for total carbon (C) and total N (Vario EL III, Germany), and three samples per plot for pH (Hanna Combo HI 98130, calibrated with 7.01 and 4.01 buffer solution, stored in KCl solution, HANNA instruments, USA). After the study, above ground biomass was harvested from all plots (Barcianicha, 29 October 2012; Giel’cykaŭ Kašyl’, 11 September 2012), oven dried at 60 °C till weight constancy, and three mixed samples per plot were analysed for total C and N.

Vegetation cover of the 70 cm × 70 cm plots was assessed in coverage classes after Peet et al. (1998). Nomenclature for vascular plants and mosses follows Rothmaler (2002), and Abramov and Volkova (1998), respectively. The nutrient status of the sites was estimated by plant species groups as indicator (Koska et al. 2001).

Water levels were measured continuously (daily averages stored) with Mini Diver data loggers (Eigenbrodt, Germany), installed in perforated tubes (inner diameter 46 mm).

One Diver was situated next to BA *Carex–Equisetum* in Barcianicha, and another in the middle between the floating tall sedge – *Typha latifolia* sites and GK *Phragmites–Lemna* in Giel'cykaŭ Kašyl'. Manual water level measurements were conducted at each site in every second to third week. Daily water levels relative to ground surface were calculated for every plot by linear regression between the continuous automatic water level time series and manually measured water levels. Because of strong peat oscillation this approach did not work for the floating sites GK *Typha–Hydrocharis* and GK *Carex–Lysimachia*. Photographic documentation (monthly during vegetation season, one time per winter, WL estimation error < 5 cm) was used here instead to reconstruct relative water levels for linear regression with Diver records.

2.3 Measurement of greenhouse gas exchange

In order to account for typical small-scale differences between vegetation types we applied a manual chamber approach to measure greenhouse gas exchange. Each of the six GHG measurement sites was equipped with three plastic collars of 70 cm × 70 cm, established in a row about 40 cm apart from each other. Each collar represents one plot. The row was East - West oriented and the North side was the working side to minimize artificial shading during measurements. Collars were inserted 15 cm deep into the peat at Barcianicha. At Giel'cykaŭ Kašyl' because of the high water level, collars were fixed on tubes orthogonally inserted into the peat and anchored in the underlying sand. Measurements were conducted from pre-installed boardwalks from August 2010 to August 2012.

CO_2 exchange was measured with transparent chambers made of plexiglas (88% light transmission, ice packs for cooling, Drösler, 2005) and opaque chambers made of grey ABS plastic covered with a white film. Both were equipped with fans for air mixing and had an inner size 72.5 cm × 72.5 cm × 51.2 cm. Opaque and transparent extensions of same area and 31.2 or 51.2 cm height with open tops were used to enlarge the chambers to accommodate for tall plants. Chambers and extensions were sealed airtight by closed cell rubber tubes attached to the bottom rims (Drösler, 2005). Carbon dioxide concentrations were measured continuously by circulating air in a closed loop between the chamber and an infrared gas analyser (LI-820, LI-COR Biosciences, USA) and recorded every five seconds by a data logger (CR200 or CR1000, Campbell Scientific, USA). Simultaneously, air temperature inside and outside the chamber, and PAR were recorded automatically ("109" temperature probes protected by radiation

sheets, SKP215, Campbell Scientific, USA), while soil temperatures were measured manually in 2, 5, and 10 cm depth once per chamber measurement with Pro-DigiTemp insertion thermometers (Carl Roth, Germany). For CO_2 measurements bright or hardly cloudy days were selected to capture the complete PAR range from zero to solar noon. During the one-day measurement campaigns eight to ten transparent chamber measurements of two to three minutes were carried out on each plot from dawn until late afternoon. Measurements were equally distributed over the daily range of PAR to determine light response of gross primary production (GPP). A similar number of opaque chamber measurements of 3–5 min were performed over the same period to capture the temperature response of ecosystem respiration (R_{eco}). Measurement campaigns were repeated every third to fourth week to account for seasonal changes in water table depth and plant development.

CH_4 and N_2O fluxes were measured once every second to third week during the snow free period and monthly during winter using non-air mixed opaque chambers, of the same material as the other opaque chambers, but shaped as a truncated pyramid (inner size at bottom 72.5 cm × 72.5 cm, inner size at top 62.5 cm × 62.5 cm, height 51.2 cm). Four to five air samples were taken from the chamber headspace during a 15–20 min enclosure and subsequently analysed in the laboratory with a gas chromatograph (Chromatec-Cristal 5000.2, Chromatec, Russia), using an electron capture detector (ECD) for analysing N_2O and a flame ionization detector (FID) for CH_4, and an auto-sampler (Loftfield, Germany). From August 2010 to August 2012 a total of 36 CH_4 and N_2O as well as 26 CO_2-measuring campaigns were carried out at every site.

Diurnal CH_4 emission dynamics and the effect of chamber transparency and headspace mixing were additionally studied at one plot per site by frequent CH_4 measurements for one to two summer days, using alternately two (opaque and transparent, both with fan) or three (opaque and transparent with and opaque without fan) chamber types (for details cf. Minke et al., 2014).

Parameters for the development of flux models were recorded on site during GHG-measurement campaigns, and monitored continuously by nearby climate stations (BA: Višnieva, 5.6 km NW of Barcianicha, and GK: Z'dzitava, 6.3 km NE of Giel'cykaŭ Kašyl'). At the stations soil temperatures in 2 and 5 cm depth, and air temperature 20 cm above surface were measured with "109" temperature probes (Campbell Scientific, USA). Photosynthetically active radiation (PAR) was monitored using a SKP215 Quantum Sensor, precipitation with 52202 Raingauge Heated European, atmospheric pressure with CS100 Setra Barometric Sensor, and all data were recorded half-hourly

with CR200 data loggers (all devices from Campbell Scientific, USA). Regression between site and climate station temperature data was subsequently applied to derive continuous half-hourly time series for each site. Due to technical problems with the rain gauges precipitation data were received from Gidrometcentr, Belarus, from the weather stations in Valožyn (15 km E of Barcianicha) and Pružany (54 km WNW of Giel'cykaŭ Kašyl'). Data from both weather stations of Gidrometcentr were also used to calculate 30 year (1979–2008) monthly averages of air temperature and precipitation.

2.4 Calculation of flux rates, annual emission models and uncertainties

2.4.1 Carbon dioxide

The net ecosystem exchange (NEE, the CO_2 flux between the ecosystem and the atmosphere) is the balance between CO_2 inputs to the ecosystem by gross primary production (GPP) and CO_2 losses by ecosystem respiration (R_{eco}; Alm et al., 1997; Chapin et al., 2002). A positive sign refers to a flux from the ecosystem to the atmosphere, a negative sign to an ecosystem sink (cf. Falge et al., 2001). Annual NEE rates were modelled for each plot separately based on the plot and campaign specific relationships between R_{eco} and temperature, as well as between GPP and PAR.

Modeling NEE using the approach of Hoffmann et al. (2015) resulted in surprisingly high annual net CO_2 uptake rates of the *Phragmites australis* sites. To check for possible impacts of the calculation routine on the result we used alternatively the approach of Leiber-Sauheitl et al. (2014) and arrived at slightly smaller CO_2 sinks. Both approaches are reasonable, build on the same assumptions but differ with respect to flux estimation, reference temperature, GPP model and importance of the significance of the model fits, as described in the following paragraphs. To avoid that modelled CO_2 exchange rates would be biased by specific features of only one of the approaches, both approaches were used to model annual CO_2 exchange rates and their means were taken as final estimates. However, for simplicity we only present modelled CO_2 time series derived by the Hoffmann (H)-approach.

Calculation of measured CO_2 flux rates

Measured CO_2 flux rates were calculated in both approaches as linear CO_2 concentration change in the chamber over time. Measurements were discarded if PAR

fluctuated by > ± 10% (transparent chambers) and chamber temperature > ± 0.75 K (transparent and opaque chambers) from the mean of the selected flux calculation interval. In the H-approach a moving window of variable time was applied to adjust the starting point and length of the regression sequence according to the regression quality. The optimal flux length was selected in a second step, based on the minimum Akaike Information Criterion (AIC) of the flux fit to the R_{eco} or the GPP functions. In the Leiber-Sauheitl (LS)–approach a moving window of constant length (one minute for all except for two minutes for opaque flux measurements at *Phragmites australis* plots because of large chamber volumes and slow concentration changes) was used to select the regression sequence with maximum R^2 and minimum variance. If maximum R^2 resulted in different fluxes than minimum variance (46% of all flux measurements) the mean of both was used as flux estimate.

Modelling of half-hourly CO_2 exchange rates

In both approaches the Lloyd and Taylor (1994) equation (Eq. 1) was fitted to R_{eco} flux data against site temperatures for each plot and campaign.

$$R_{eco} = R_{ref} \times \exp\left[E_0 \times \left(\frac{1}{T_{ref} - T_0} - \frac{1}{T - T_0} \right) \right] \quad (1)$$

R_{eco} = ecosystem respiration (mg CO_2−C m^{-2} h^{-1}), R_{ref} = R_{eco} at reference temperature (mg CO_2−C m^{-2} h^{-1}), E_0 = activation energy like parameter (K), T_{ref} = reference temperature (283.15 K), T_0 = temperature constant for the start of biological processes: (227.13 K), T = soil or air temperature during measurement of best fit with the dataset (K).

In the H-approach Eq. (1) was fitted to R_{eco} flux rates separately for air temperature and soil temperatures and the final R_{eco} parameter pairs were selected out of all significant ($p \leq 0.1$) sets based on the lowest AIC. If parameterization was not significant or failed, or if the daily temperature amplitude was below 3 K, the average CO_2 flux of the measurement campaign was used. In the LS-approach one R_{eco} fit per plot and campaign was calculated against air temperatures. If parameterization was impossible or the temperature amplitude was below 2 K, the mean campaign R_{eco} flux was used.

In a second step GPP fluxes were determined by subtracting modelled R_{eco} fluxes from timely corresponding, measured NEE flux rates. In the H-approach a rectangular hyperbola equation (Michaelis-Menten, 1913; Eq. 2) was fitted to the relation between

PAR and GPP flux rates to calibrate GPP parameter sets of α (initial slope of the curve; light use efficiency) and GP_{max} (rate of carbon fixation for infinite PAR).

$$GPP = \frac{\alpha \times PAR \times GP_{\max}}{\alpha \times PAR + GP_{\max}} \quad (2)$$

GPP parameter pairs with lowest AIC were selected from each campaign out of all significant regression parameters ($p \leq 0.1$). If the parameter estimation failed, a non rectangular hyperbolic equation was fitted to the data (Gilmanov et al., 2007). If this failed, too, an average parameter approach was used. Assuming declining GPP fluxes when PAR drops from 500 to 0 µmol m^{-2} s^{-1} α was set -0.01 and GP_{max} estimated as the mean campaign GPP flux. In the LS-approach the modified Michaelis-Menten model of Falge et al. (2001; Eq. 3) was applied and GP2000 was calculated instead of GP_{max}, i.e. the rate of carbon fixation at PAR of 2000 µmol m^{-2} s^{-1}. Campaigns for which no GPP fit was found were skipped.

$$GPP = \frac{\alpha \times PAR \times GP2000}{GP2000 + \alpha \times PAR - \frac{GP2000}{2000} \times PAR} \quad (3)$$

Based on the GPP parameter pairs and continuously monitored PAR data, GPP was modelled in both approaches for each plot at a temporal resolution of 30 min. NEE was subsequently calculated as the difference between GPP and R_{eco}.

Uncertainty, accuracy, and variability

Model performance for the interpolation between the measurement campaigns was estimated for the H-approach by leave-one-out cross-validation. Stepwise one measurement campaign was left out after the other and the modelled R_{eco} and NEE fluxes were compared with the measured fluxes in the left out campaigns. Model performance was assessed by the Nash–Sutcliffe efficiency (NSE, Moriasi et al., 2007). The random error of the annual CO_2 balances was calculated for the H-approach using the R-script Version 1.1 of Hoffmann et al. (2015). Campaign specific confidence intervals (p = 0.01) were determined for the temperature models, as well as for the R_{eco} and GPP parameter pairs by bootstrapping. Subsequently 100 samples were taken randomly from the confidence intervals and used to compute R_{eco}, GPP, and NEE models. The random error of the CO_2 models calculated with the H-approach represents the model uncertainty at the days of the measurement campaigns, but not of the interpolation. As indicated by the differences between the H and LS approaches the

uncertainty of the annual balances is larger. To arrive at more realistic error estimates we accounted for the random error and for the difference between both approaches and defined the confidence intervals as the difference between the annual sums of both approaches plus two times the annual random error calculated for the H-approach..

2.4.2 Methane and nitrous oxide

Calculation of fluxes

Methane fluxes were estimated with the R package "flux 0.2–1" (Jurasinski et al., 2012) using linear regression. For normalized root mean square error (NRMSE) < 0.2 the flux with the largest number of concentration measurements was preferred. If NRMSE ≥ 0.2 a set of fluxes was estimated using the maximum number up to at least three concentration measurements. Subsequently the flux with the lowest NRMSE was selected.. Fluxes were accepted if NRMSE < 0.4, R^2 ≥ 0.8 and n ≥ 3. This was the case in 639 out of 686 methane flux measurements, with 477 accepted fluxes based on n ≥ 4.

Nitrous oxide flux rates and their standard deviations were calculated with linear regression using the same air samples as accepted for CH_4 flux calculation.

Modelling of emissions

Methane fluxes correlated with some environmental factors. This allowed to develop a univariate nonlinear regression model for daily methane fluxes. The relatively small number of observations did not allow any multivariate approaches. First, the relation between environmental factors (air temperature, soil temperature, water level, air pressure, PAR, GPP, R_{eco}, NEE) and measured CH_4 fluxes was tested for each plot using non-parametric Spearman's correlation to identify the strongest driving parameter. Second, several published nonlinear regression models (Eqs. 1, 4, 5) were fitted to the relation between methane emissions and the driver and the optimal model was selected based on the AIC.

The strongest Spearman's ρ correlations were found between methane fluxes and instantaneous on site soil temperature (median ρ for two years and all 18 plots = 0.85, n = 36), followed by half-hourly and daily R_{eco} (both 0.83), half-hourly GPP (−0.80; both modelled with the H-approach), and on site air temperature (0.75). Mean daily site specific soil temperatures, calculated by linear regression between site measurements

and climate station data, also correlated well with methane fluxes (median ρ per plot and year = 0.85) and had a strong covariance with other factors. Water level did not correlate significantly with methane emissions at any plot, possibly because it was always close to or above the surface. Therefore mean daily soil temperature was chosen as the single driving factor for modelling methane emission.

The temperature dependency of methane production and emission was previously described by the Arrhenius function or its logarithmic form (Conrad et al., 1987; Schütz et al., 1990; Daulat and Clymo, 1998; Kim et al., 1998)

$$F = A \times e^{\frac{-E}{R \times T}} \quad (4)$$

F = flux rate of CH_4 (mg CH_4 −C m^{-2} h^{-1}), A = Arrhenius parameter (mg CH_4 −C m^{-2} h^{-1}), E = apparent activation energy (J mol^{-1}), R = gas constant (8.314 J mol^{-1} K^{-1}), T = soil temperature (K).

Also an exponential function or its logarithmic form has been widely applied to calculate methane emission in relation to temperature (Dise and Gorham, 1993; Saarnio et al., 1997; Kettunen et al., 2000; Tuittila et al., 2000; Laine et al., 2007; Rinne et al., 2007; Wilson et al., 2009):

$$F = a \times e^{b \times T} \quad (5)$$

F = flux rate of CH_4 (mg CH_4 −C m^{-2} h^{-1}), a = flux rate at T = 0 °C (mg CH_4 −C m^{-2} h^{-1}), b = coefficient ($°C^{-1}$), T = soil temperature (°C).

The third tested function was the Lloyd and Taylor (1994) equation for soil respiration (Eq. 1, Sect. 2.4.1).

We used the AIC to select from Eqs. (1), (4), and (5) the one that best fitted to our data set. The differences were small but the AIC of the Lloyd and Taylor equation (Eq. 1) was the smallest for 33 out of 36 fits (fits for 2 years and 18 plots) and was therefore chosen to model methane emissions for all plots and years.

As N_2O fluxes did not correlate with recorded environmental factors annual emissions were estimated by linear interpolation between measurements.

Uncertainty, accuracy, and variability

Model performance was tested by leave-one-out cross-validation.

Errors of modelled annual methane emissions were calculated using Monte Carlo simulation in four steps. We included the uncertainty of the temperature transfer from the climate station to the site, the uncertainty of the measured flux rates, and the

parameter uncertainty of the Lloyd and Taylor fits. Temperature uncertainty was quantified by 1000 times repeated bootstrapped re-sampling of site and station temperatures with the same indices. Second, a set of 1000 normally distributed flux values was generated for every flux measurement based on the calculated CH_4 flux rates and their standard deviation. Third, each of the 1000 soil temperature data set was paired with one of the 1000 flux data sets and 1000 Lloyd and Taylor fits (Eq. 1) were performed. Fourth, from each of the Lloyd and Taylor fits 1000 bootstrap parameter samples were created using bootstrap of the residuals (Efron, 1979; Leiber-Sauheitl et al., 2014). More than 99% of the bootstrap fits were successful what resulted in more than 990000 parameter pairs per plot and year. Finally, 1000 Lloyd and Taylor fits were randomly sampled from the parameter pairs, combined with the 1000 soil temperature data set and used to calculate 1000 methane models per plot and year. For each time point and the annual sums 95% and 5% quantiles were calculated to construct confidence intervals of the time series and annual gas balances. As the CH_4 model fits include the temperature and methane flux uncertainties over the entire year, the 90% confidence intervals do to some extent also account for the interpolation between measurement days.

Uncertainties of annual N_2O fluxes were calculated solely based on estimates and standard deviations of the measured fluxes. 1000 normally distributed values of each flux were generated and linearly interpolated. This resulted in 1000 annual emission estimates per plot and year, but the calculated 90% confidence intervals represent only the uncertainties of the measured fluxes.

2.5 Statistical analyses

Correlations between annual balances of CH_4 and CO_2 with site factors were tested using the non-parametric Spearman's ρ.

Differences of daytime methane fluxes among chamber types were analysed using either the Mann–Whitney test or the Kruskal–Wallis test with the post-hoc nonparametric Tukey-type multiple comparison procedure developed by Nemenyi (Zar, 1999).

3 Results

3.1 Site conditions

Most of the residual peat at both peatlands was very slightly to moderately decomposed radicel peat (Table 1). Surface peat was eutrophic and acid at both study sites, but less decomposed at Barcianicha as compared to Giel'cykaŭ Kašyl' (Table 1) .Barcianicha had 27 to 76 cm thick layers of brown moss peat about 40 cm below surface, while for Giel'cykaŭ Kašyl' notable amounts of *Phragmites* macrofossils were found in the upper 100 to 140 cm of the profile.

Vegetation was homogeneous within sites types at Barcianicha and varied little between years (Table A1). Vegetation indicated mesotrophic conditions at Barcianicha (Koska et al., 2001). At Giel'cykaŭ Kašyl' species cover was homogeneous among plots and years for GK *Phragmites–Lemna* (Table A1). The floating sites GK *Carex–Lysimachia* and GK *Typha–Hydrocharis* constituted a strongly interweaved fine mosaic of sedge tussocks and cattail and shared many species. Vegetation indicated eutrophic conditions for Giel'cykaŭ Kašyl' (Koska et al., 2001).

Mean annual temperature at Barcianicha was 6.5 °C in the first and 6.9 °C in the second measurement year, close to the long term mean (6.4 °C, 1979–2008). Annual precipitation in the first year (740 mm) was higher than the long-term mean (665 mm) due to heavy summer rains (Fig. 2a), but lower (633 mm) in the second.

Giel'cykaŭ Kašyl' (Fig. 2b) was generally warmer and drier than Barcianicha (long-term mean 7.3 °C and 594 mm, respectively, 1979–2008). Also here the first year was wetter (804 mm) and the second year drier (500 mm) and annual temperatures were close to the long term mean (7.3 °C in the first year; 7.9 °C in the second year)..

Annual water levels relative to the surface at Barcianicha decreased in the order BA *Phragmites–Carex* (14 ± 2 cm above surface), BA *Carex–Equisetum* and BA *Eriophorum–Carex* (at surface; Table 1). Differences among plots within sites were small (Figs. 4c, 4d, and 4e). Annual values for both years were the same (Table 1). Summer and winter median water levels were very similar, despite temporal fluctuations of up to 18 cm.

Water tables at GK *Phragmites–Lemna* (Giel'cyka˘u Kašyl') were about one metre in the first year, and dropped to about 70 cm above surface in the second year (Table 1). At the close by floating tall sedge – *Typha latifolia* reed sites water levels were only about 10 cm above the surface and the drop from the first to the second year was small, both because of the oscillating peat surface. Summer water levels were lower than winter levels, but never dropped significantly below surface (Table 1, Figs. 4n and 4o). Annual

water levels varied more among plots than at Barcianicha, with a maximum of 11 cm at GK *Phragmites–Lemna* (Fig. 4p).

Above ground biomass harvested in autumn 2012 at Barcianicha (Table 1) was largest for BA *Phragmites–Carex* (296 ± 79 g C m^{-2}), lower for BA *Eriophorum–Carex* (117 ± 34 g C m^{-2}) and smallest for BA *Carex–Equisetum* (55 ± 22 g C m^{-2}). Biomass harvests of GK *Typha-Hydrocharis* and GK *Carex-Lysimachia* were similar to BA *Phragmites–Carex*, but that of GK *Phragmites–Lemna* were two times larger (586 ± 121 g C m^{-2}, Table 1). The doubled biomass production of *Phragmites australis* at Giel'cykaŭ Kašyl' compared to Barcianicha supports the nutrient rich conditions, probably resulting from different water supply (river and grassland drainage water for GK, groundwater for BA) and different land use history (after peat extraction temporary grassland before rewetting of GK, rewetting directly after peat extraction of BA).

3.2 Carbon dioxide emissions

Model performance tested for the H-approach was good for both years and all site types and plots. Cross-validation resulted in a median NSE of 0.78 (range from 0.38 to 0.90) for the R_{eco} models and of 0.76 (0.21 to 0.91) for the NEE models.

All sites of Barcianicha were net CO_2 sinks in the first year. NEE was −528 (90% confidence interval -933, -194) g CO_2−C m^{-2} yr^{-1} for BA *Phragmites–Carex*, -86 (-130, -38) g CO_2−C m^{-2} yr^{-1} for BA *Eriophorum–Carex* and −88 (-114, -68) g CO_2−C m^{-2} yr^{-1} for *Carex–Equisetum* (Fig. 5, Table 2). In the second year, resulting from increased R_{eco} and decreased GPP, the net CO_2 uptake decreased. NEE of BA *Phragmites–Carex* dropped to −329 (-431, -220) g CO_2−C m^{-2} yr^{-1}, BA *Eriophorum–Carex* became CO_2 neutral and BA *Carex–Equisetum* turned into a small source of 24 (-6, 55) g CO_2−C m^{-2} yr^{-1}.

Both, sinks and sources were larger at the Giel'cykaŭ Kašyl' sites. NEE of GK *Phragmites–Lemna* was −611 (−819, −450) g CO_2−C m^{-2} yr^{-1} in the first and, despite of increasing R_{eco} fluxes, −1175 (−1567, −690) g CO_2−C m^{-2} yr^{-1} in the second year. The high values were attributed to extremely high annual GPP reaching −2267 (−2733, −1843) g CO_2−C m^{-2} yr^{-1} in the second year, equivalent to twice the R_{eco} fluxes (Fig. 5, Tab. 3). At the other Giel'cykaŭ Kašyl' sites R_{eco} and GPP also increased from the first to the second year, but R_{eco} and GPP largely balanced each other. GK *Typha–Hydrocharis* consequently varied between a source of 151 (41, 300) g CO_2−C m^{-2} yr^{-1} in the first and a sink of −113 (−418, 66) g CO_2−C m^{-2} yr^{-1} in the second year. GK

Carex–Lysimachia was a net CO_2 source in both years, releasing 166 (66, 252) g CO_2−C m^{-2} yr^{-1} in the first and 216 (48, 470) g CO_2−C m^{-2} yr^{-1} in the second year.

On average the net CO_2 sink at Barcianicha decreased in the second year by 130 g CO_2−C m^{-2} yr^{-1} or 56% but increased at Giel'cykaŭ Kašyl' by 259 g CO_2−C m^{-2} yr^{-1} or 263% compared to the first year.

Small scale spatial variability of annual NEE fluxes was largest for GK *Phragmites–Lemna* (187 ± 153 g CO_2-C m^{-2} yr^{-1}, mean ± standard deviation of the absolute differences between annual plot emissions and annual site emissions, *n*=6; Table 3; Fig. 5). Absolute within site spatial variability of NEE exchange rates was lower for BA *Phragmites–Carex,* GK *Carex–Lysimachia* and GK *Typha–Hydrocharis* and small for BA *Eriophorum–Carex* and BA *Carex–Equisetum* (16 ± 13 and 9 ± 5 g CO_2-C m^{-2} yr^{-1}; Table 3, Fig. 5). The order of sites changes, when within site variability of NEE is related to annual site NEE fluxes. Relative variability was the same for BA *Carex–Equisetum* and GK *Phragmites–Lemna* (19 ± 12% and 20 ± 11%, respectively, Table 3). This is related to the importance of the annual flux magnitude as illustrated by BA *Eriophorum–Carex* in the second year that resulted from an annual site NEE of -7 g CO_2-C m^{-2} yr^{-1} and an absolute within site spatial variability of 11 g CO_2-C m^{-2} yr^{-1} in a relative variability of 152%.

3.3 Methane emissions

3.3.1 Diurnal variability of methane emissions and impact of chamber types

Opaque and transparent chambers slightly differed in the development of air temperature and relative humidity of the headspace during the measurements. Despite cooling temperature rose more in transparent (up to 3 ± 0.5 °C, mean ± standard error; Table A2) than in opaque chambers (up to 1.4 ± 0.2 °C). Due to cooling, however, relative humidity increased less in transparent (up to 18.1 ± 3.7%) than in opaque chambers (up to 14.8 ± 2.3%). Differences were significant at few measurement days only (Table A2)..

Pronounced diurnal methane emission dynamics were observed for BA *Phragmites–Carex* and GK *Phragmites–Lemna*, much stronger than for any other site (Fig. 3). Significantly different methane emissions between opaque and transparent chambers, however, were only found for GK *Typha–Hydrocharis* and GK *Carex–Lysimachia* (Table A2). Measurements with transparent chambers resulted here in 20% and 10% higher

emission estimates than with opaque chambers with fan. Also for BA *Eriophorum–Carex* I measurements with transparent chambers produced 9% higher flux rates than opaque chambers, but the difference was not significant (Fig. 3, Table A2). At all other sites the flux rates measured with transparent and opaque chambers with fan agreed within 2%. The chamber intercomparison suggests a potential reduction of convective gas transport in *Typha latifolia* by shading with the regularly applied opaque chambers without fan. Consequently, the measured growing season fluxes from GK *Typha–Hydrocharis* and GK *Carex–Lysimachia.* were corrected upwards by 20% as *Typha latifolia* was present at all plots except for GK *Carex-Lysimachia* I in 2012 where the diurnal chamber intercomparison took place (Table A2). Fluxes from the other sites were not corrected because chamber effects were not significant.

3.3.2 Annual methane emissions

The Lloyd–Taylor methane models performed well for all sites except for the second year of BA *Phragmites–Carex* and GK *Phragmites–Lemna*. NSE for all but the *Phragmites australis* sites ranged between 0.38 and 0.85 (median 0.58). Models of the *Phragmites australis* sites were acceptable in the first year (median NSE 0.37, range 0.05 to 0.82) but performed worse in the second year (median 0.01, range -0.25 to 0.24) where models did not adequately capture the seasonal course of methane emissions at three out of nine *Phragmites* plots. Models of GK *Phragmites–Lemna* III and BA *Phragmites–Carex* III did not explain the high emissions in August 2011 (Figs. 4h and 4s). Both and the model of BA *Phragmites–Lemna* I overestimated emissions in spring and early summer 2012. Annual emissions were calculated alternatively by linear interpolation for the second year of BA *Phragmites–Lemna* I and III and GK *Phragmites–Lemna* III. The resulting flux rates of 25, 28, and 118 g CH_4−C m^{-2} yr^{-1} lie within the 90% confidence intervals of the temperature driven Lloyd–Taylor methane model (30, 32, and 139 g CH_4−C m^{-2} yr^{-1}; Table A3). The Lloyd–Taylor models were therefore accepted despite of negative NSE.

GK *Phragmites–Lemna* had the highest methane emissions of all sites, estimated to 100 (90% confidence interval 48, 147) and 101 (61, 177) g CH_4−C m^{-2} yr^{-1} in the first and second year, respectively (Table 2). GK *Carex–Lysimachia* released less methane. GK *Typha–Hydrocharis* was the smallest source among the studied sites at Giel'cykaŭ Kašyl' with 60 (47, 77) and 68 (52, 92) g CH_4−C m^{-2} yr^{-1}, but still larger than the Barcianicha sites.

BA *Phragmites–Carex* emitted 42 (28, 58) in the first and 36 (22, 52) g CH_4−C m^{-2} yr^{-1} in the second year. BA *Carex–Equisetum* was a much smaller methane source, but the absolute lowest annual methane emissions were found at BA *Eriophorum–Carex* being 10 (9, 13) in the first and 11 (10, 14) g CH_4−C m^{-2} yr^{-1} in the second year (Table 2).

Methane emissions of all sites hardly differed between years (Table 2). They decreased in the second year at Barcianicha by on average 3 g CH_4−C m^{-2} yr^{-1} or 14% but increased at Giel'cykaŭ Kašyl' by 4 g CH_4−C m^{-2} yr^{-1} or 5% compared to the first year. Absolute and relative small scale variability of methane emissions tended to increase with annual methane emission height (Fig. 5, Table 3).

3.4 Nitrous oxide emissions

Emissions of N_2O from all plots were around zero (Fig. 5e and f). Maximum plot emissions were around 0.5 g N_2O−N m^{-2} yr^{-1}, but were usually compensated for by similar large uptakes in a neighbour plot or the other year. The overlap of the 90% confidence of all sites, plots and years indicates that N_2O emissions were not significantly different among them.

3.5 Correlations between annual GHG emissions and site parameters

GHG emissions were only weakly related to surface peat characteristics. Spearman's ρ of the correlation between annual methane emissions and C/N ratio was −0.50* and between annual net CO_2 exchange and pH 0.40' (' $P \leq 0.05$; * $P \leq 0.01$, $n = 36$; i.e. correlation of peat characteristics of 18 plots with annual fluxes of these plots of two GHG measuring years).

Median annual water level was not correlated with R_{eco}, but with NEE and CH_4 emissions and most strongly with GPP (Fig. 6). Correlations of water levels with R_{eco}, GPP, NEE and CH_4, were highly significant when the floating sites GK *Typha–Hydrocharis* and GK *Carex–Lysimachia* were excluded from the analysis (Fig. 6, ρ in brackets). Correlations of water level with NEE and CH_4 were also strong for Barcianicha alone (ρ = −0.60**, 0.85***, respectively, ** $P \leq 0.001$; *** $P \leq 0.0001$, n = 18).

Total above ground biomass carbon harvested after the second measuring year strongly correlated with the second year annual balances of CH_4, R_{eco} and GPP, but not with NEE (Fig. 6). Without the floating tall sedge – *Typha latifolia* sites correlations

between biomass and balances of R_{eco} and GPP were stronger and the correlation between biomass and NEE became highly significant. When only Barcianicha was analysed, correlation between biomass and methane emissions where not significant, but correlations between biomass and R_{eco}, GPP, and NEE were strong (ρ = 0.98***, −0.98***, −0.95**, respectively, n = 9).

Annual CH_4 emissions did not correlate with annual NEE, but strongly with R_{eco} and GPP (Fig. 6). Excluding GK *Typha–Hydrocharis* and GK *Carex–Lysimachia* resulted in highly significant correlation between methane and NEE (Fig. 6, ρ = −0.83, P < 0.0001, n = 30). For Barcianicha alone correlation between NEE and CH_4 emissions was also significant (ρ = −0.67, P = 0.0028, n = 18).

As expected, within-site variation of R_{eco} and absolute GPP generally scaled with biomass. (Fig. 6). Methane emissions increased among plots of BA *Phragmites–Carex* with increasing absolute GPP and R_{eco} and all three fluxes were positively correlated with above ground biomass. A positive correlation between biomass and methane also occurred for GK *Carex–Lysimachia*, while at GK *Phragmites–Lemna* methane emissions tended to decrease with increasing net CO_2 uptake (Fig. 6).

3.6 Carbon and GHG-balances of sites

Both *Phragmites* sites were surprisingly strong carbon sinks (Table 2) but also methane sources and had only low net GHG emissions with an overall mean of 1.3 t CO_2 eq ha^{-1} yr. The two years average GHG balances of the shallowly flooded, mesotrophic site BA *Phragmites–Carex* and the deeply inundated, eutrophic site GK *Phragmites–Lemna* were −1.7 (90% confidence interval -15.0, 10.2) and 4.2 (-26.8, 37.7) t CO_2 eq ha^{-1} yr^{-1}, respectively. The mesotrophic small sedge reeds BA *Eriophorum–Carex* and BA *Carex–Equisetum* with water tables around the land surface were weak carbon sinks and methane sources (Table 2). Both sites were small net GHG emitters of 2.3 (-1.0, 5.6) and 4.2 (2.1, 6.8) t CO_2 eq ha^{-1} yr^{-1}, respectively. The eutrophic, floating tall sedge – *Typha latifolia* reeds were, despite of shallow relative water depths, strong methane sources and in most years also net CO_2 emitters. GK *Typha–Hydrocharis* was a substantial GHG source of 25.1 (9.5, 37.9) t CO_2 eq ha^{-1} yr^{-1} and GK *Carex–Lysimachia* even emitted 39.1 (26.6, 58.0) t CO_2 eq ha^{-1} yr^{-1}.

The role of N_2O exchange was negligible for the GHG-balances of all sites.

4 Discussion

4.1 Annual CO_2 and methane balances

Contrary to our hypothesis (i) only three sites were stable net CO_2 sinks, two sites switched between sink and source and one site was a net CO_2 source in both years. Surprisingly, both eutrophic tall sedge - *Typha latifolia* reeds on newly formed floating mats were net CO_2 sources over the two year period although the mats suggest a net carbon accumulation since rewetting.

For all site years with a net CO_2 sink we can argue in line with hypothesis (i) that peat loss by oxidation has stopped after rewetting. We suggest that also in site years with a net CO_2 source the CO_2 loss originated from decaying plant material rather than from peat. All source sites were fully water-saturated throughout the year and had substantial methane emissions, indicating fully anaerobic conditions. We suggest that the CO_2 originated from accumulated plant litter or from high stress related plant respiration as the sites where CO_2 sources occurred were characterized by transitional vegetation stages (see below).

The CO_2 and methane balances of the mesotrophic small sedge reeds at Barcianicha agree with the literature. Eutrophic tall sedge - *Typha latofilia* reeds on newly formed floating mats have not been studied before but results generally agree with literature from eutrophic mineral reed ecosystems. The *Phragmites* reeds also agree with literature with regard to the methane emissions, but have an exceptionally strong CO_2 sink. In the following details are discussed for the three site groups.

Annual methane emissions from BA *Eriophorum–Carex* and BA *Carex–Equisetum* were of the same magnitude as from similar small sedge reeds in two rewetted cutover Atlantic bogs (Wilson et al., 2009, 2013). Net uptake and net release of CO_2, however, was smaller for BA *Eriophorum–Carex* and BA *Carex–Equisetum* as compared to the mentioned Irish sites (Wilson et al., 2007, 2013; Table 6), perhaps partly resulting from lower productivity.

Methane emissions from BA *Phragmites–Carex* compared well to the shallow water inner reed zone (33 g CH_4−C m^{-2} yr^{-1}) and that from GK *Phragmites-Lemna* to the deep water outer reed zone (122 g CH_4−C m^{-2} yr^{-1}) of lake Lake Vesijärvi in Southern Finland (Table 6; Kankaala et al., 2004). Methane emissions from a *Phragmites australis* dominated, shallowly inundated marsh in north-central Nebraska, USA (60 g CH_4−C m^{-2} yr^{-1}; Kim et al., 1998) as well as from wet *Phragmites australis* stands in a rewetted Dutch fen (88 g CH_4−C m^{-2} yr^{-1}; Hendriks et al., 2007) were between both

Phragmites reeds of the present study. Annual NEE fluxes of both *Phragmites australis* sites were more than ten times higher than at a freshwater tidal reed wetland in NE China, though above ground biomass was comparable (Zhou et al., 2009). The differences result from smaller ratios of R_{eco} to GPP in the present (0.58 ± 0.09, n = 4) compared to the tidal reed study (0.95) and can be explained by permanent inundation of BA *Phragmites–Carex* and GK *Phragmites–Lemna*, and consequently low heterotrophic respiration, while the soil of the tidal reed wetland was periodically aerated. The importance of water level was also evident for a *Phragmites australis* site in a rewetted former grassland fen in NE Germany that sequestrated 83 g CO_2−C m^{-2} yr^{-1} and emitted 11 g CH_4−C m^{-2} yr^{-1} in an exceptionally wet year (WL at surface) but released 68 g CO_2−C m^{-2} yr^{-1} and only 1 g CH_4−C m^{-2} yr^{-1} in a typical year (WL below surface; Günther et al., 2014).

Annual methane and CO_2 fluxes from floating tall sedge – *Typha latifolia* reeds are not reported in the literature. Methane emissions from GK *Typha–Hydrocharis* and GK *Carex–Lysimachia* were higher compared to a pristine, water saturated sedge fen (dominated by *Carex aquatilis*) in the southern Rocky Mountains (30 to 34 g CH_4−C m^{-2} yr^{-1}; Table 6; Wickland et al., 2001) or to *Carex acutiformis and Typha latifolia* sites during the wet year in the above mentioned rewetted fen grassland (47 and 10 g CH_4−C m^{-2} yr^{-1}, respectively; Günther et al., 2014). They were comparable to temperate *Typha latifolia* (82 g CH_4−C m^{-2} yr^{-1}; Whiting and Chanton, 2001) and *T. angustifolia* marshes (51 g CH_4−C m^{-2} yr^{-1}, Chu et al., 2015; 127 g CH_4−C m^{-2} yr^{-1}, Strachan et al., 2015). The constantly high water levels made us expect a net CO_2 uptake at GK *Typha–Hydrocharis* and GK *Carex–Lysimachia*, as was found for *Typha latifolia* and *T. angustifolia* marshes (Whiting and Chanton, 2001; Strachan et al., 2015), for a water saturated temperate sedge fen in the Czech Republic (Dušek et al., 2012), and in the wet year for *Carex acutiformis and Typha latifolia* (Günther et al., 2014). However, in contrast to our first hypothesis the sites GK *Typha–Hydrocharis* and GK *Carex–Lysimachia* were net CO_2 sources. Similar, a wet sedge fen in the southern Rocky Mountains (Wickland et al., 2001) and a water saturated *Typha angustifolia* marsh (Chu et al., 2015) were found to be CO_2 sources (Table 6). Chu et al. (2015) explain their findings by abnormal climatic conditions. As climatic conditions during the first year of the present study were similar to the long term average, other factors, like reduced GPP because of shading from old standing leaves (Rocha et al., 2008) may have been important, as there was much dry biomass present. Also the high water levels and their strong fluctuations may have imposed stress on the vegetation (Dušek et al., 2012), as

indicated by changes in the cover of the dominant species between years (Table A1) and the early aging of the sedges. High R_{eco} fluxes from the floating tall sedge – *Typha latifolia* reeds could be the result of increased maintenance respiration because of environmental stress (Chapin et al., 2002) combined with high heterotrophic respiration from decomposing dead plant material which formed the main part of the sedge tussocks (estimated from photographic documentation). This indicates that the plant communities were not well adapted to the present conditions and represent a transient development stage.

4.2 Robustness of annual GHG balances

4.2.1 Methane

Overall, our measurement design and data treatment produces annual methane balances at the high end of the expected real fluxes.

The pronounced diurnal methane emission dynamics from BA *Phragmites–Carex* and GK *Phragmites–Lemna* with fivefold flux increases from morning to midday result from active air transport in *Phragmites australis* aerenchyma in the growing season driven by sun light (Armstrong and Armstrong, 1991; Brix et al., 1992; Armstrong et al., 1996). In contrast to other studies (Van der Nat and Middelburg, 2000; Günther et al., 2013) we did not find a significant impact of chamber transparency on measured methane emission rates, maybe because enclosed plants were connected by rhizomes with culms outside the chamber. Such connection seems to allow for pressure propagation and continuation of unrestrained convective gas flow (Juutinen et al., 2004; Minke et al., 2014). Consequently the application of opaque chambers has not biased annual emission estimates from the *Phragmites australis* sites.

Day-to-day variability and seasonal variation of average daily emissions from *Phragmites australis* stands are controlled by sediment temperature (Kim et al., 1998; Kankaala et al., 2004), which supports our decision to use soil temperature for modelling methane emissions. However, a single measurement at any time during daylight does not represent the daily emission average. For the monitored days (Fig. 3) most measurements between 9.00 and 18.00 h resulted in equal or higher estimates as compared to the 24 hour mean. Our daylight measurements during the growing period slightly overestimate the daily methane flux rates. In summary, our approach tended to overestimate the real emissions at the *Phragmites australis* sites.

GK *Typha–Hydrocharis* showed less pronounced diurnal methane emission dynamics (Fig. 3). Unlike *Phragmites*, *Typha latifolia* reacted on shading. The reduction of emissions by opaque chambers agrees with other studies of *Typha latifolia* (Chanton et al., 1993; Whiting and Chanton, 1996). Similar to *Phragmites australis*, green parts of *Typha latifolia* pressurize during daylight which drives convective gas transport and accelerates methane efflux (Brix et al., 1992; Whiting and Chanton, 1996). Obviously, *Typha latifolia* plants are less connected than *Phragmites* and cannot compensate for small scale shading during chamber deployment. Our transparent/opaque ratios of measured methane flux rates of 1.2 agrees with previous studies for *Typha latifolia* (1.1 – Whiting and Chanton, 1996; 1.3 – Günther et al., 2013). However, we do not know the variability of the ratio under different weather conditions. We applied the correction factor 1.2 for total daily methane emissions during the growing season, although chamber transparency only matters during daylight. Estimated annual emissions will consequently be at the high end of real emissions from the site.

Methane measurements were significantly affected by shading at the floating *Carex elata* plot, but not at the small sedge plots dominated by *Carex rostrata* and *Eriophorum angustifolium*. Gas transport in sedges is driven only by diffusion (Armstrong, 1979; King et al., 1998). Existing studies were ambiguous regarding the effect of shading by chambers. Shading reduced methane emissions from *Carex aquatilis* (Morrissey et al., 1993) and *Carex allivescers* (Hirota et al., 2004), but not from *Carex limosa* and *Carex rostrata* (Whiting and Chanton, 1992), *Carex acutiformis* (Günther et al., 2013) and *Eriophorum angustifolium* (Joabsson et al., 1999, Whiting and Chanton, 1992).

4.2.2 Carbon dioxide

The two approaches used to model CO_2 exchange rates resulted in very similar annual balances. Plot-wise annual R_{eco} calculated with the H-approach was on average 5 ± 5% (mean ± standard deviation, n = 36) below the LS-approach, while GPP sink was 1 ± 3% (n = 36) higher. Resulting annual net CO_2 uptake was consequently on average stronger for the H-approach than for the LS-approach. The mean difference of NEE between both approaches was 43 ± 41 g CO_2−Cm^{-2} yr^{-1} (n = 36). This indicates that measured fluxes and general modelling assumptions, i.e. the temperature relation of R_{eco} and PAR relation of GPP were robust towards differences in flux calculation and

model parameterization. Also the good results of the cross validations of the models of the H-approach at all sites indicate a high robustness of the results.

The net annual CO_2 sink of the *Phragmites australis* sites was surprisingly large, especially at GK *Phragmites–Lemna*. The first year NEE of this site agreed with the estimate of Brix et al. (2001; Table 6) but the second year uptake was twice as high. To test for plausibility we roughly estimated the carbon flux partitioning in the ecosystem from independent data. Based on dry weight of green above ground biomass assessed at the end of the growing seasons 2011 and 2012 and on published ratios between above ground and below ground biomass production we estimated the net annual primary production (NPP, g C m^{-2} yr^{-1}) of the *Phragmites australis* sites during both GHG measurement periods (Table 5). Using NPP, NEE, and GPP we estimated heterotrophic and autotrophic respiration (R_h and R_a, Table 5) and evaluated their meaningfulness. As expected because of inundation, heterotrophic respiration was low, ranging between 77 and 114 g CO_2−Cm^{-2} yr^{-1}. The ratios of heterotrophic respiration to methane emissions (CO_2-C / CH_4-C) were 2.2 and 2.3 in the first an second year, respectively for BA *Phragmites–Carex* and closer, 1.0 and 1.1 for GK *Phragmites–Lemna*. Similar ratios were found in incubation experiments for organic bottom sediments and the upper peat layer of a flooded former fen grassland (Hahn-Schöfl et al., 2011). Calculated autotrophic respiration was half of GPP, but differed considerably between years (43 to 61%). This range is plausible given the uncertainty of the underlying estimates (especially of NPP), as the efficiency of converting GPP to NPP is generally assumed to be relatively constant (cf. Chapin et al., 2002). In summary, the carbon partitioning test was plausible and supports the exceptional net CO_2 uptake in the *Phragmites* sites. Such uptake may be explained by strong rhizome formation in a relatively young reed ecosystem but may not represent a long-term equilibrium.

4.3 Controls of annual GHG emissions

Reality proved more complex than our hypotheses. We studied transient vegetation development stages after fen rewetting, which may not necessarily be generalized to equilibrium stages. The findings related to the hypotheses are as follows:

(i) The annual CO_2 balance was best explained by vegetation biomass, which includes the role of vegetation composition and species. *Phragmites* reeds were by far the most productive ecosystems at both studied peatlands. The nutrient status affected

productivity, but species effects dominated the CO_2 balance. Inundation depth had no systematic effect on the annual CO_2 balance.

(ii) Methane emissions were site specific. They increased with productivity and correlated strongly with R_{eco} fluxes. Methane was obviously most driven by biological activity of vegetation and soil organisms. Continuously inundated sites tended to have higher methane emissions than sites where water levels remained near the land surface.

(iii) Under mesotrophic conditions rewetting leads to stable small net GHG sources or even sinks because methane emissions are largely balanced by the net CO_2 sink. Under eutrophic conditions, rewetted fens remain net GHG sources in most cases. Vegetation types can be sinks or sources of CO_2 and emit substantial amounts of methane so that rewetting effects on the GHG balance remain difficult to predict.

(iv) We reject, however, that the CO_2 sink and methane emissions peak under shallow inundation. In contrast, the various vegetation types with shallow water showed strongly diverging CO_2, methane and GHG balances in a small water level range.

The high GHG emissions from the floating tall sedge – *Typha latifolia* reeds are comparable to deep-drained temperate fen grassland (26 t CO_2 eq ha^{-1} yr^{-1} – Drösler et al., 2014; 65 t CO_2 eq ha^{-1} yr^{-1} – Eickenscheidt et al., 2015). In contrast to the other sites of the present study, important targets of peatland rewetting, i.e. restoration of the carbon sink function and reduction of GHG emissions have not been achieved for GK *Typha–Hydrocharis* and GK *Carex–Lysimachia*.

In the following we discuss the background for the revision of the hypotheses, reasons for the differences among sites and the individual drivers of the GHG fluxes.

4.3.1 Water table

In a meta-analysis Blain et al. (2014) found that methane emissions from boreal and temperate, undrained and rewetted peatlands tend to increase but the CO_2 sink to decrease along a water level gradient from 30 cm below to 20 cm above surface. The water level in our study ranged from 3 cm below to 104 cm above surface with most sites within 10 cm water table range. The diverse vegetation types with roughly similar water table had widely diverging CO_2, methane and GHG balances that we cannot confirm any trend. In drained peatlands water table position defines the depth of the aerobic zone and consequently the rate of peat oxidation (Blain et al., 2014, Couwenberg et al., 2011). The sites of the present study, however, were permanently water saturated and water levels affect CO_2 fluxes most likely indirectly via other

controlling factors, for example vegetation composition. Methane emissions under flooded conditions are hardly affected by water table position (Blain et al., 2014). When aerenchymous plants are abundant, as in the present study, they dominate the gas exchange and methane bypasses the oxygenated water column (Whiting and Chanton, 1992; Chanton and Whiting, 1995). In analogy to CO_2, water level has affected methane emissions of the studied sites mainly indirectly by vegetation composition and the type and abundance of aerenchymous plants.

Near-zero nitrous oxide emissions at all sites agree with other studies from rewetted fens with permanent water saturation (Hendriks et al., 2007; Wilson et al., 2013).

4.3.2 Nutrient conditions

The different nutrient status of the studied peatlands cannot be explained by surface peat properties, which were both eutrophic, but by water supply (river and grassland drainage water for Giel'cykaŭ Kašyl', groundwater for Barcianicha). Eutrophic conditions supported the establishment of more productive plant species at Giel'cykaŭ Kašyl' compared to the mesotrophic Barcianicha, higher productivity of *Phragmites australis* and higher microbial activity indicated by higher R_{eco} and methane fluxes. This is in line with Blain et al. (2014) who found that methane and CO_2 emissions are higher from rich temperate rewetted fens as compared to poor fens and bogs. Our results indicate that rich temperate rewetted fens may be further subdivided into mesotrophic and eutrophic to account for significantly different methane emissions.

4.3.3 Vegetation and plant productivity

Plant productivity was the main control of CO_2 fluxes, as indicated by the strong correlation between biomass and NEE for all sites except GK *Typha–Hydrocharis* and GK *Carex–Lysimachia* (Fig. 6). However, also differences of methane emissions within sites increased with above ground biomass and GPP (Fig. 6), and were larger in Giel'cykaŭ Kašyl' compared to Barcianicha, and in both peatlands for the *Phragmites australis* sites (Table 3). This is most likely due to control of vegetation and plant productivity on methane emissions, as indicated by the highly significant correlation between methane emissions and biomass, and can be explained by supply of organic material and by plant mediated gas exchange (Whiting and Chanton, 1993; Chanton et al., 1995; Bellisario et al., 1999; Whalen, 2005).

Fresh organic substrates were rather limited at Barcianicha, as indicated by the thin layer of litter and many bare peat patches. More emissions can be expected when more litter accumulates (Waddington and Day, 2007). Plant litter was more abundant at Giel'cykaŭ Kašyl', certainly because of higher plant productivity, but also because of a longer period since rewetting and deeper inundation. This may explain why a strong correlation between NEE and methane emissions was found at Barcianicha, but not at Giel'cykaŭ Kašyl'. Methane production did not only depend on actual primary production, especially in the floating tall sedge – *Typha latifolia* reeds of Giel'cykaŭ Kašyl'. Methane emissions from GK *Typha–Hydrocharis* and GK *Carex–Lysimachia* were high and, similar to the large R_{eco} fluxes, at least partly fuelled by old litter. Also allochthonous carbon can not be excluded as a substrate for methane production at Giel'cykaŭ Kašyl' (Chu et al., 2015), for example from floating plants like *Lemna trisulca* that form detritus with a much higher methane production potential compared to *Phragmites australis* litter (Kankaala et al., 2003).

The zone of floating mats will most likely continue for many years to emit large amounts of methane and only a shift towards *Phragmites australis* dominated plant communities with larger CO_2 sink potentials seems to allow for reduction of GHG emissions. Such a shift may not be unlikely, because *Phragmites australis* is growing on most of the area of Giel'cykaŭ Kašyl' and has been abundant at GK *Typha–Hydrocharis* and GK *Carex–Lysimachia* in former times, as indicated by macrofossils in the peat profile (Table 1).

5 Conclusions

The eutrophic peatland Giel'cykaŭ Kašyl' with deep standing water had a large carbon sink potential, but also a high risk of local net CO_2 losses. The site varied spatially and temporally between being a small net GHG sink and a large GHG source because of high methane emissions. The mesotrophic peatland Barcianicha with shallow, constant water levels, in contrast, constituted a smaller but more stable carbon sink and only a small GHG source. Both net CO_2 uptake and methane emissions were strongly linked to vegetation and plant productivity, which in turn were related to water level and nutrient conditions. Emission variability increased with productivity of sites. This implies that the formulation of robust emission factors for high-productive vegetation types and mire ecosystems requires more long-term and spatially resolved GHG emission studies than for low-productive ones.

Unexpectedly high carbon losses and GHG emissions from the floating tall sedge – *Typha latifolia* reeds of Giel'cykaŭ Kašyl' were most likely caused by vegetation suffering from high and strongly fluctuating water levels. The exact sources of these high emissions, as well as the duration and successional pathway of the supposed transitional phase require further investigation.

Our study indicates that permanent, shallow inundation of cutover temperate fens is a suitable measure to arrive at low GHG emissions. *Phragmites australis* establishment should be promoted in deeper flooded areas and will lead to comparably moderate, but variable GHG emissions or even occasional sinks. The study supports previous findings for rewetted peatlands that the risk of high GHG emissions is higher for eutrophic than mesotrophic peatlands. In spite of the possible high emissions in some vegetation types or years, flooding of eutrophic fens still represents a safe GHG mitigation option for temperate fens because even the hotspot of our study, the eutrophic floating mats, did not exceed typical GHG emissions from drained fen grasslands and the spatially dominant flooded *Phragmites australis* reed emitted by far less GHG than drained fens.

Acknowledgements. This study was funded by the KfW Entwicklungsbank in the framework of the International Climate Initiative of the German Federal Ministry for the Environment, Nature Conservation and Nuclear Safety (BMU) under BMU project Reference No.: II. C. 53, and by the Centre for International Migration and Development (CIM) and the Royal Society for the Protection of Birds (RSPB). We thank APB – BirdLife Belarus and the National Academy of Sciences of Belarus for creating ideal research conditions, Hans Joosten for support in designing the study and for commenting the manuscript, Nadzeya Liashchynskaya, Hanna Grabenberger, Aleksandr Novik, Nikolaj Belovezhkin, Konstantin Timokhov and Aleksandr Pavlyuchenko for help in the field, Sergej Zui for construction and maintenance of measuring equipment, Vyacheslav Rakovich for showing us Barcianicha, Petr Boldovskij, Vadim Protasevich and the students and teachers of the school of Z'dzitava for warm welcome, logistical support and information on land use history, Michel Bechthold for advice on evaluation of the hydrological data, Roland Fuß, Katharina Leiber-Sauheitl and Thomas Leppelt for consultations on statistical issues.

References

Abramov, I. I. and Volkova, L. A.: Handbook of Mosses of Karelia, KMK Scientific Press Delphos, Moscow, 1998.

AG Boden: Bodenkundliche Kartieranleitung (Soil survey manual), 5th Edn., Hannover, 2005.

Alm, J., Talanov, A., Saarnio, S., Silvola, J., Ikkonen, E., Aaltonen, H., Nykänen, H., and Martikainen, P. J.: Reconstruction of the carbon balance for microsites in a boreal oligotrophic pine fen, Finland, Oecologia, 110, 423–431, 1997.

Armstrong, J. 5 and Armstrong, W.: A convective through–flow of gases in *Phragmites australis* (Cav.) Trin. Ex Steud., Aquat. Bot., 39, 75–88, 1991.

Armstrong, J., Armstrong, W., Beckett, P. M., Halder, J. E., Lythe, S., Holt, R., and Sinclair, A.: Pathways of aeration and the mechanisms and beneficial effects of humidity and Venturi induced convections in *Phragmites australis* (Cav.) Trin. Ex Steud., Aquat. Bot., 54, 177–198, 10, 1996.

Armstrong, W.: Aeration in higher plants, Adv. Bot. Res., 7, 236–332, 1979.

Asaeda, T., Manatunge, J., Roberts, J., and Hai, D. N.: Seasonal dynamics of resource translocation between the aboveground organs and age-specific rhizome segments of *Phragmites australis*, Environ. Exp. Bot., 57, 9–18, 2006.

Bellisario, L. M., Bubier, J. L., Moore, T. R., and Chanton, J. P.: Controls on CH_4 emissions from a northern peatland, Global Biogeochem. Cy., 13, 81–91, 1999.

Beyer, C. and Höper, H.: Greenhouse gas exchange of rewetted bog peat extraction sites and a *Sphagnum* cultivation site in northwest Germany, Biogeosciences, 12, 2101–2117, doi:10.5194/bg-12-2101-2015, 2015.

Blain, D., Murdiyarso, D., Couwenberg, J., Nagata, O., Renou-Wilson, F., Sirin, A., Strack, M., Tuittila, E.-S., Wilson, D., Evans, C. D., Fukuda, M., and Parish, F.: Chapter 3: Rewetted organic soils, in: 2013 Supplement to the 2006 IPCC Guidelines for National Greenhouse Gas Inventories: Wetlands, edited by: Hiraishi, T., Krug, T., Tanabe, K., Srivastava, N., Baasansuren, J., Fukuda, M., and Troxler, T. G., IPCC, Switzerland, 3.1–3.42, 2014.

Brix, H., Sorrell, B. K., and Orr, P. T.: Internal pressurization and convective gas flow in some emergent freshwater macrophytes, Limnol. Oceanogr., 37, 1420–1433, 1992.

Brix, H., Sorrell, B. K., and Lorenzen, B.: Are *Phragmites*-dominated wetlands a net source or net sink of greenhouse gases?, Aquat. Bot., 69, 313–324, 2001.

Chanton, J. P. and Whiting, G. J.: Trace gas exchange in freshwater and coastal marine environments: ebullition and transport by plants, in: Biogenic Trace Gases: Measuring Emissions from Soil and Water, edited by: Matson, P. A. and Harriss, R. C., Blackwell Science Ltd., Oxford, UK, 98–125, 1995.

Chanton, J. P., Whiting, G., Happell, J., and Gerard, G.: Contrasting rates and diurnal patterns of methane emission from different types of vegetation, Aquat. Bot., 46, 111–128, 1993.

Chanton, J. P., Bauer, J. E., Glaser, P. A., Siegel, D. I., Kelley, C. A., Tyler, S. C., Romanowicz, E. H., and Lazrus, A.: Radiocarbon evidence for the substrates supporting methane formation within northern Minnesota peatlands, Geochim. Cosmochim. Ac., 59, 3663–3668, 1995.

Chapin III, F. S., Matson, P. A., and Mooney, H. A.: Principles of Terrestrial Ecosystem Ecology, Springer-Verlag, New York, 2002.

Chu, H., Gottgens, J. F., Chen, J., Sun, G., Desai, A. R., Ouyang, Z., Shao, C., and Czajkowski, K.: Climatic variability, hydrologic anomaly, and methane emission can turn productive freshwater marshes into net carbon sources, Glob. Change Biol., 21, 1165–1181, doi:10.1111/gcb.12760, 2015.

Conrad, R., Schütz, H., and Babbel, M.: Temperature limitation of hydrogen turnover and methanogenesis in anoxic paddy soil, FEMS Microbiol. Ecol., 45, 281–289, 1987.

Couwenberg, J., Augustin, J., Michaelis, D., and Joosten, H.: Emission Reductions from Rewetting of Peatlands, Towards a Field Guide for the Assessment of Greenhouse Gas Emissions from Central European Peatlands, Duene/RSPB, Greifswald/Sandy, 2008.

Couwenberg, J., Thiele, A., Tanneberger, F., Augustin, J., Bärisch, S., Dubovik, D., Liashchynskaya, N., Michaelis, D., Minke, M., Skuratovich, A., and Joosten, H.: Assessing greenhouse gas emissions from peatlands using vegetation as a proxy, Hydrobiologia, 674, 67–89, doi:10.1007/s10750-011-0729-x, 2011.

Daulat, W. E. and Clymo, R. S.: Effects of temperature and watertable on the efflux of methane from peatland surface cores, Atmos. Environ., 32, 3207–3218, 1998.

Dise, N. B., Gorham, E., and Verry, E. S.: Environmental factors controlling methane emissions from peatlands in Northern Minnesota, J. Geophys. Res., 98, 10583–10594, 1993.

Drösler, M.: Trace Gas Exchange and Climatic Relevance of Bog Ecosystems, southern Germany, Ph.D. thesis, Technische Universität München, München, 2005.

Drösler, M., Freibauer, A., Christensen, T. R., and Friborg, T.: Observations and status of peatland greenhouse gas emissions in Europe, in: The Continental-Scale Greenhouse Gas Balance of Europe, edited by: Dolman, H., Valentini, R., and Freibauer, A., Ecol. Stud., 203, 243–261, 2008.

Drösler, M., Verchot, L. V., Freibauer, A., Pan, G., Evans, C. D., Bourbonniere, R. A., Alm, J. P., Page, S., Agus, F., Hergoualc'h, K., Couwenberg, J., Jauhiainen, J., Sabiham, S., Wang, C., Srivastava, N., Borgeau-Chavez, L., Hooijer, A., Minkkinen, K., French, N., Strand, T., Sirin, A., Mickler, R., Tansey, K., and Larkin, N.: Chapter 2: Drained inland organic soils, in: 2013 Supplement to the 2006 IPCC Guidelines for National Greenhouse Gas Inventories: Wetlands, edited by: Hiraishi, T., Krug, T., Tanabe, K., Srivastava, N., Baasansuren, J., Fukuda, M., and Troxler, T. G., IPCC, Switzerland, 2.1–2.76, 2014.

Dušek, J., Žížková, H., Stellner, S., Czerný, R., and Květ, J.: Fluctuating water table affects gross ecosystem production and gross radiation use efficiency in a sedge-grass marsh, Hydrobiologia, 692, 57–66, doi:10.1007/s10750-012-0998-z, 2012.

Eickenscheidt, T., Heinichen, J., and Drösler, M.: The greenhouse gas balance of a drained fen peatland is mainly controlled by land-use rather than soil organic carbon content, Biogeosciences, 12, 5161–5184, doi:10.5194/bg-12-5161-2015, 2015.

Efron, B.: Bootstrap methods: Another look at the jackknife, Ann. Stat., 7, 1–26, 1979.

Falge, E., Baldocchi, D., Olson, R., Anthoni, P., Aubinet, M., Bernhofer, C., Burba, G., Ceulemans, R., Clement, R., Dolman, H., Granier, A., Gross, P., Grünwald, T., Hollinger, D., Jensen, N.-O., Katul, G., Keronen, P., Kowalski, A., Lai, C. T., Law, B. E., Meyers, T., Moncrieff, J., Moors, E., Munger, J. W., Pilegaard, K., Rannik, Ü., Rebmann, C., Suyker, A., Tenhunen, J., Tu, K., Verma, S., Vesala, T., Wilson, K., and Wofsy, S.: Gap filling strategies or defensible annual sums of net ecosystem exchange, Agr. Forest Meteorol., 107, 43–69, 2001.

Gilmanov, T. G., Soussana, J. F., Aires, L., Allard, V., Ammann, C., Balzarolo, M., Barcza, Z., Bernhofer, C., Campbell, C. L., Cernusca, A., Cescatti, A., Clifton-Brown, J., Dirks, B. O. M., Dore, S., Eugster, W., Fuhrer, J., Gimeno, C., Gruenwald, T., Haszpra, L., Hensen, A., Ibrom, A., Jacobs, A. F. G., Jones, M. B., Lanigan, G., Laurila, T., Lohila, A., Manca, G., Marcolla, B., Nagy, Z., Pilegaard, K., Pinter, K., Pio, C., Raschi, A., Rogiers, N., Sanz, M. J., Stefani, P., Sutton, M., Tuba, Z., Valentini, R., Williams, M. L., and Wohlfahrt, G.: Partitioning European grassland net ecosystem CO_2 exchange into gross primary productivity and ecosystem respiration using light response function analysis, Agric. Ecosyst. Environ., 121, 93–120, 2007.

Günther, A., Jurasinski, G., Huth, V., and Glatzel, S.: Opaque closed chambers underestimate methane fluxes of *Phragmites australis* (Cav.) Trin. ex Steud., Environ. Monit. Assess., 186, 2151–2158, doi:10.1007/s10661-013-3524-5, 2013.

Günther, A., Huth, V., Jurasinski, G., and Glatzel, S.: The effect of biomass harvesting on greenhouse gas emissions from a rewetted temperate fen, GCB Bioenergy, 7, 1092–1106, doi:10.1111/gcbb.12214, 2014.

Hahn-Schöfl, M., Zak, D., Minke, M., Gelbrecht, J., Augustin, J., and Freibauer, A.: Organic sediment formed during inundation of a degraded fen grassland emits large fluxes of CH_4 and CO_2, Biogeosciences, 8, 1539–1550, doi:10.5194/bg-8-1539-2011, 2011.

Hendriks, D. M. D., van Huissteden, J., Dolman, A. J., and van der Molen, M. K.: The full greenhouse gas balance of an abandoned peat meadow, Biogeosciences, 4, 411–424, doi:10.5194/bg-4-411-2007, 2007.

Hirota, M., Tang, Y., Hu, Q., Hirata, S., Kato, T., Mo, W., Cao, G., and Mariko, S.: Methane emissions from different vegetation zones in a Qinghai-Tibetan Plateau wetland, Soil Biol. Biochem., 36, 737–748, 2004.

Hoffmann, M., Jurisch, N., Albiac, B. E., Hagemann, U., Drösler, M., Sommer, M., and Augustin, J.: Automated modeling of ecosystem CO2 fluxes based on periodic closed chamber measurements: a standardized conceptual and practical approach, Agr. Forest Meteorol., 200, 30–45, 2015.

Joabsson, A., Christensen, T. R., and Wallén, B.: Influence of vascular plant photosynthetic rate on CH_4 emission from peat monoliths from southern boreal Sweden, Polar Res., 18, 215–220, 1999.

Joosten, H. and Clarke, D.: Wise Use of Mires and Peatlands – Background and Principles Including a Framework for Decision-Making, Saarijärvi, International Mire Conservation Group and International Peat Society, 2002.

Joosten, H., Tapio-Biström, M.-L., and Tol, S.: Peatlands – Guidance for Climate Change Mitigation by Conservation, Rehabilitation and Sustainable Use, FAO and Wetlands International, Rome, 2012.

Jurasinski, G., Koebsch, F., and Hagemann, U.: Flux: Flux Rate Calculation from Dynamic Closed Chamber Measurements, R Package Version 0.2-1, Rostock, 2012.

Juutinen, S., Alm, J., Larmola, T., Saarnio, S., Martikainen, P. J., and Silvola, J.: Stand-specific diurnal dynamics of CH_4 fluxes in boreal lakes: patterns and controls, J. Geophys. Res., 109, D19313, doi:10.1029/2004JD004782, 2004.

Kadastrovyj spravochnik “Torfyanoj fond Belorusskoj SSR” (Cadastral reference “Peat fond of the BSSR”), Minsk, 1979.

Kankaala, P., Käki, T., and Ojala, A.: Quality of detritus impacts on spatial variation of methane emissions from littoral sediment of a boreal lake, Arch. Hydrobiol., 157, 47–66, 2003.

Kankaala, P., Ojala, A., and Käki, T.: Temporal and spatial variation in methane emissions from a flooded transgression shore of a boreal lake, Biogeochemistry, 68, 297–311, 2004.

Kettunen, A., Kaitala, V., Alm, J., Silvola, J., Nykänen, H., and Martikainen, P. J.: Predicting variations in methane emissions from boreal peatlands through regression models, Boreal Environ. Res., 5, 115–131, 2000.

Kim, J., Verma, S. B., and Billesbach, D. P.: Seasonal variation in methane emission from a temperate *Phragmites*-dominated marsh: effect of growth stage and plant mediated transport, Glob. Change Biol., 5, 433–440, 1998.

King, J. Y., Reeburgh, W. S., and Regli, S. K.: Methane emission and transport by arctic sedges in Alaska: results of a vegetation removal experiment, J. Geophys. Res., 103, 29083–29092, 1998.

Knox, S. H., Sturtevant, C., Matthes, J. H., Koteen, L., Verfaillie, J., and Baldocchi, D.: Agricultural peatland restoration: effects of land-use change on greenhouse gas (CO_2 and CH_4) fluxes in the Sacramento-San Joaquin Delta, Glob. Change Biol., 21, 750–765, 2015.

Koebsch, F., Glatzel, S., Hofmann, J., Forbrich, I., and Jurasinski, G.: CO_2 exchange of a temperate fen during the conversion from moderately rewetting to flooding, J. Geophys. Res.-Biogeo., 118, 940–950, doi:10.1002/jgrg.20069, 2013.

Köppen, W.: Das geographische System der Klimate, in: Handbuch der Klimatologie, Vol. IC, edited by: Köppen, W. and Geiger, R., Borntraeger, Berlin, C1–C44, 1936.

Koska, I., Succow, M., Clausnitzer, U., Timmermann, T., and Roth, S.: Vegetationskundliche Kennzeichnung von Mooren (topische Betrachtung), in: Landschaftsökologische Moorkunde, edited by: Succow, M. and Joosten, H., Schweizerbart, Stuttgart, 112–184, 2001.

Kottek, M., Grieser, J., Beck, C., Rudolf, B., and Rubel, F.: World map of the Köppen–Geiger climate classification up–dated, Meteorol. Z., 15, 259–263, 2006.

Kozulin, A., Tanovitskaya, N., and Vershitskaya, I.: Methodical Recommendations for Ecological Rehabilitation of Damaged Mires and Prevention of Disturbance to the Hydrological Regime of Mire Ecosystems in the Process of Drainage, Scientific and Practical Centre for Bio Resources, Institute for Nature Management of the National Academy of Sciences of Belarus, 2010.

Laine, A., Wilson, D., Kiely, G., and Byrne, K. A.: Methane flux dynamics in an Irish lowland blanket bog, Plant Soil, 299, 181–193, doi:10.1007/s11104-007-9374-6, 2007.

Leiber-Sauheitl, K., Fuß, R., Voigt, C., and Freibauer, A.: High CO_2 fluxes from grassland on histic Gleysol along soil carbon and drainage gradients, Biogeosciences, 11, 749–761, doi:10.5194/bg-11-749-2014, 2014.

Lloyd, J. and Taylor, J. A.: On the temperature dependence of soil respiration, Funct. Ecol., 8, 315–323, 1994.

Maksimenkov, M. V., Pugachevskij, A. V., and Rakovich, V. V.: Nauchnoe Obosnovanie povtornogo zabolachivaniya vyrabotannogo torfyanogo mestorozhdeniya “Bortenikha” (Scientific justification of rewetting of the cutaway peatland “Barcianicha”), The Forest Ministry of the Republic of Belarus, Minsk, 2006.

Michaelis, L. and Menten, M. L.: Die Kinetik der Invertinwirkung, Biochem. Z., 49, 333–369, 25 1913.

Minayeva, T., Sirin, A., and Bragg, O. (Eds.): A Quick Scan of Peatlands in Central and Eastern Europe, Wetlands International, Wageningen, 2009.

Minke, M., Augustin, J., Hagemann, U., and Joosten, H.: Similar methane fluxes measured by transparent and opaque chambers point at belowground connectivity of *Phragmites australis* beyond the chamber footprint, Aquat. Bot., 113, 63–71, 2014.

Moriasi, D. N., Arnold, J. G., Van Liew, M. W., Binger, R. L., Harmel, R. D., and Veith, T.: Model evaluation guidelines for systematic quantification of accuracy in watersheds simulations, T. ASABE, 50, 885–900, 2007.

Morrissey, L. A., Zobel, D. B., and Livingston, G. P.: Significance of stomatal control on methane release from *Carex*-dominated wetlands, Chemosphere, 26, 339–355, 1993.

Myhre, G., Shindell, D., Bréon, F.-M., Collins, W., Fuglestvedt, J., Huang, J., Koch, D., Lamarque, J.-F., Lee, D., Mendoza, B., Nakajima, T., Robock, A., Stephens, G., Takemura, T., and Zhang, H.: Anthropogenic and natural radiative forcing, in: Climate Change 2013: The Physical Science Basis, Contribution of Working Group I to the Fifth Assessment Report of the Intergovernmental Panel on Climate Change, edited by: Stocker, T. F., Qin, D., Plattner, G.-K., Tignor, M., Allen, S. K., Boschung, J., Nauels, A., Xia, Y., Bex, V., and Midgley, P. M., Cambridge University Press, Cambridge, UK, New York, NY, USA, 659–740, 2013.

Peet, R. K., Wentworth, T. R., and White, P. S.: A flexible, multipurpose method for recording vegetation composition and structure, Castanea, 63, 262–274, 1998.

Rinne, J., Riutta, T., Pihlatie, M., Aurela, M., Haapanala, S., Tuovinen, J.-P., and Tuittila, E.-S.: Annual cycle of methane emission from a boreal fen measured by the eddy covariance technique, Tellus B, 59, 449–457, 2007.

Rocha, A. V. and Goulden, M. L.: Large interannual CO_2 and energy exchange variability in a freshwater marsh under consistent environmental conditions, J. Geophys. Res., 113, G04019, doi:10.1029/2008JG000712, 2008.

Rocha, A. V., Potts, D. L., and Goulden, M. L.: Standing litter as a driver of interannual CO_2 exchange variability in a freshwater marsh, J. Geophys. Res., 113, G04020, doi:10.1029/2008JG000713, 2008.

Rothmaler, W.: Exkursionsflora von Deutschland: Kritischer Band (Flora of Germany), 9th edn., Spektrum, Heidelberg, Berlin, 2002.

Saarnio, S., Alm, J., Silvola, J., Lohila, A., Nykänen, H., and Martikainen, P. J.: Seasonal variation in CH_4 emissions and production and oxidation potentials at microsites on an oligotrophic pine fen, Oecologia, 110, 414–422, 1997.

Samaritani, E., Siegenthaler, A., Yli-Petäys, M., Buttler, A., Christin, P.-A., and Mitchell, E. A. D.: Seasonal net ecosystem carbon exchange of a regenerating cutaway bog: how long does it take to restore the C-sequestration function?, Restor. Ecol., 19, 480–489, doi:10.1111/j.1526-100X.2010.00662.x, 2011.

Scarton, F., Day, J. W., and Rismondo, A.: Above and belowground production of *Phragmites australis* in the Po Delta, Italy, Boll. Mus. civ. St. nat. Venezia, 49, 213–222, 1999.

Schierup, H. H.: Biomass and primary productivity in a *Phragmites communis* Trin. swamp in North Jutland, Denmark, Verh. Internat. Verein. Limnol., 20, 93–99, 1978, cited in: Westlake, D. F.: The primary productivity of water plants, in: Studies on Aquatic Vascular Plants, edited by: Symoens, J. J., Hooper, S. S., and Compère, P., Royal Botanical Society of Belgium, Bruessls, 165–180, 1982.

Schütz, H., Seiler, W., and Conrad, R.: Influence of soil temperature on methane emission from rice paddy fields, Biogeochemistry, 11, 11–95, 1990.

Soetaert, K., Hoffmann, M., Meire, P., Starink, M., Van Oevelen, D., Van Regenmortel, S., and Cox, T.: Modeling growth and carbon allocation in two reed beds (*Phragmites australis*) in the Scheldt estuary, Aquat. Bot., 79, 211–234, 2004.

Soini, P., Riutta, T., Yli-Petäys, M., and Vasander, H.: Comparison of vegetation and CO_2 dynamics between a restored cut-away peatland and a pristine fen: evaluation of the restoration success, Restor. Ecol., 18, 894–903, doi:10.1111/j.1526-100X.2009.00520.x, 2010.

Strachan, I. B., Nugent, K. A., Crombie, S., and Bonneville, M.-C.: Carbon dioxide and methane exchange at a cool-temperate freshwater marsh, Environ. Res. Lett., 10, 065006, doi:10.1088/1748-9326/10/6/065006, 2015.

Strack, M. and Zuback, Y. C. A.: Annual carbon balance of a peatland 10 yr following restoration, Biogeosciences, 10, 2885–2896, doi:10.5194/bg-10-2885-2013, 2013.

Tanneberger, F. and Wichtmann, W. (Eds.): Carbon Credits from Peatland Rewetting, Climate – Biodiversity – Land Use, Science, Policy, Implementation and Recommendations of a Pilot Project in Belarus, Schweizerbart, Stuttgart, 2011.

Tanovitskaya, N. and Kozulin, A.: Peatlands in Belarus, in: Carbon Credits from Peatland Rewetting, Climate – Biodiversity – Land Use, Science, Policy, Implementation and Recommendations of a Pilot Project in Belarus, edited by: Tanneberger, F. and Wichtmann, W., Schweizerbart, Stuttgart, 3–12, 2011.

Thiele, A., Edom, F., and Liashchynskaya, N.: Prediction of vegetation development with and without rewetting, in: Carbon Credits from Peatland Rewetting, Climate – Biodiversity – Land Use, Science, Policy, Implementation and Recommendations of a Pilot Project in Belarus, edited by: Tanneberger, F. and Wichtmann, W., Schweizerbart, Stuttgart, 42–52, 2011.

Tuittila, E.-S., Komulainen, V.-M., Vasander, H., and Laine, J.: Restored cut-away peatland as a sink for atmospheric CO_2, Oecologia, 120, 563–574, 1999.

Tuittila, E.-S., Komulainen, V.-M., Vasander, H., Nykänen, H., Martikainen, P. J., and Laine, J.: Methane dynamics of a restored cut-away peatland, Glob. Change Biol., 6, 569–581, 2000.

Van der Nat, F. J. and Middelburg, J. J.: Methane emission from tidal freshwater marshes, Biogeochemistry, 49, 103–121, 2000.

Vretare, V., Weisner, 5 S. E. B., Strand, J. A., and Granéli, W.: Phenotypic plasticity in *Phragmites australis* as a functional response to water depth, Aquat. Bot., 69, 127–145, 2001.

Waddington, J. M. and Day, S. M.: Methane emissions from a peatland following restoration, J. Geophys. Res., 112, G03018, doi:10.1029/2007JG000400, 2007.

Westlake, D. F.: The primary productivity of water plants, in: Studies on Aquatic Vascular Plants, edited by: Symoens, J. J., Hooper, S. S., and Compère, P., Royal Botanical Society of Belgium, Bruessls, 165–180, 1982.

Wetlands International: Restoring Peatlands in Russia – For Fire Prevention and Climate Change Mitigation (PEATRUS), Seventh Progress Report, Submitted to KfW in August 2015.

Whalen, S. C.: Biogeochemistry of methane exchange between natural wetlands and the atmosphere, Environ. Eng. Sci., 22, 73–94, 2005.

Whiting, G. J. and Chanton, J. P.: Plant-dependent CH_4 emission in a subarctic Canadian fen, Global Biogeochem. Cy., 6, 225–231, 1992.

Whiting, G. J. and Chanton, J. P.: Primary production control of methane emission from wetlands, Nature, 367, 794–795, 1993.

Whiting, G. J. and Chanton, J. P.: Control of diurnal pattern of methane emission from aquatic macrophytes by gas transport mechanisms, Aquat. Bot., 54, 237–253, 1996.

Whiting, G. J. and Chanton, J. P.: Greenhouse carbon balance of wetlands: methane emission versus carbon sequestration, Tellus B, 53, 521–528, 2001.

Wickland, K.: Carbon gas exchange at a southern Rocky Mountain wetland, 1996–1998, Global Biogeochem. Cy., 15, 321–335, 2001.

Wilson, D., Tuittila, E.-S., Alm, J., Laine, J., Farrell, E. P., and Byrne, K. A.: Carbon dioxide dynamics of a restored maritime peatland, Ecoscience, 14, 71–80, 2007.

Wilson, D., Alm, J., Laine, J., Byrne, K. A., Farrell, E. P., and Tuittila, E.-S.: Rewetting of cutaway peatlands: are we re-creating hot spots of methane emissions?, Restor. Ecol., 17, 796–806, doi:10.1111/j.1526-100X.2008.00416.x, 2009.

Wilson, D., Farrell, C., Mueller, C., Hepp, S., and Renou-Wilson, F.: Rewetted industrial cutaway peatlands in western Ireland: a prime location for climate change mitigation?, MaP, 11, 1–22, 2013.

Yili-Petäys, M., Laine, J., Vasander, H., and Tuittila, E.-S.: Carbon gas exchange of a revegetated cut-away peatland five decades after abandonment, Boreal Environ. Res., 12, 177–190, 2007.

Zak, D., Reuter, H., Augustin, J., Shatwell, T., Barth, M., Gelbrecht, J., and McInnes, R. J.: Changes of the CO_2 and CH_4 production potential of rewetted fens in the perspective of temporal vegetation shifts, Biogeosciences, 12, 2455–2468, doi:10.5194/bg-12-2455-2015, 2015.

Zar, J. H.: Biostatistical Analysis, Prentice Hall, Upper Saddler River, 1999.

Zhou, L., Zhou, G., and Jia, Q.: Annual cycle of CO_2 exchange over a reed (*Phragmites australis*) wetland in Northeast China, Aquat. Bot., 91, 91–98, 2009.

Table 1. Site characteristics.

Site	Annual, summer, winter median water level[a] (cm above surface) 1st year	2nd year	Above Ground biomass[b] (g C m^{-2})	Surface peat pH[c]	C[d] (%)	N[d] (%)	C/N ratio	Profile description, top down[e]
BA *Eriophorum–Carex*	-3, -4, -3 ± 1	-3, -4, -1 ± 1	117 ± 34	6.2 ± 0.2	42.2 ± 1.7	2.3 ± 0.1	18.5 ± 0.2	0–9 radicel peat (H6), 9–14 silty gyttja, 14–43 radicel peat (H4, H3), 43–119 brown moss peat (H3, H4), below: middle sand
BA *Carex–Equisetum*	8, 7, 8 ± 1	8, 7, 10 ± 1	55 ± 22	6.1 ± 0.0	43.0 ± 0.2	2.6 ± 0.2	16.8 ± 1.1	0–15 radicel peat (H6), 15–30 radicel brown moss peat (H3), 30–34 *Alnus* peat (H4), 34–85 brown moss peat (H3), 85–95 clayey gyttja & coarse sand, below: fine sand
BA *Phragmites–Carex*	14, 14, 14 ± 1	14, 14, 16 ± 1	296 ± 79	6.1 ± 0.1	43.8 ± 0.3	2.7 ± 0.2	16.8 ± 1.1	0–13 lost, 13–40 radicel peat (H5/H4), 40–67 brown moss peat (H3, H4), below: gravel
GK *Typha–Hydrocharis*	10, 5, 13 ± 3	2, 0, 2 ± 3	259 ± 103	5.6 ± 0.1	41.4 ± 3.2	2.8 ± 0.2	14.8 ± 0.3	0–20 lost, 20–30 radicel peat (H5), 30–55 very highly decomposed peat with radicels (H8), 55–90 radicel peat with *Phragmites* (H5, H3), 90–103 brownmoss–radicel peat (H3), 103–113 woody radicel peat with *Phragmites* (H4), 113–140 radicel peat with *Phragmites* and brown mosses (H4), 140–150 organogyttja, below: sand
GK *Carex–Lysimachia*	10, 7, 12 ± 3	4, 2, 4 ± 3	299 ± 73	6.3 ± 0.4	43.3 ± 2.5	2.6 ± 0.4	16.7 ± 2.3	
GK *Phragmites–Lemna*	104, 86, 114 ± 6	74, 65, 75 ± 6	586 ± 121	5.7 ± 0.1	37.1 ± 4.1	2.4 ± 0.2	15.2 ± 0.5	0–10 very highly decomposed peat with radicels (H8), 10–100 radicel peat with *Phragmites* (H4, H5), 100–170 radicel peat (H5), 170–185 organogyttja, below: sand

Given are means ± standard deviations, *n* = 3 plots

[a] Summer = June-August, winter = December-Februar, [b] harvest at Barcianicha 2012-10-29, and at Giel'čykaŭ Kašyl' 2012-09-11, [c] pH (KCL) mean of three samples, [d] total carbon and nitrogen content, one sample, [e] von Post peat decomposition scale: H3 very slightly, H4 slightly, H5 moderately, H6 moderately highly, H8 very highly decomposed peat

Table 2. Annual fluxes of CO_2, CH_4, and Carbon (C balance = NEE + CH_4 emissions) with 90% confidence intervals.

Site	Year	R_{eco} (g CO_2–C m^{-2} yr^{-1})	GPP (g CO_2–C m^{-2} yr^{-1})	NEE (g CO_2–C m^{-2} yr^{-1})	CH_4 emissions (g CH_4–C m^{-2} yr^{-1})	C balance (g C m^{-2} yr^{-1})
BA *Eriophorum–Carex*	1	364 (339 to 396)	-449 (-512 to -407)	-86 (-130 to -38)	10 (9 to 13)	-75 (-114 to -30)
	2	406 (368 to 458)	-413 (-449 to -376)	-7 (-49 to 21)	11 (10 to 14)	4 (-35 to 30)
BA *Carex–Equisetum*	1	232 (196 to 262)	-320 (-361 to -279)	-88 (-114 to -68)	17 (13 to 22)	-71 (-92 to -56)
	2	327 (282 to 371)	-302 (-334 to -281)	24 (-6 to 55)	13 (9 to 16)	37 (8 to 66)
BA *Phragmites–Carex*	1	614 (478 to 737)	-1141 (-1595 to -888)	-528 (-933 to -194)	42 (28 to 58)	-486 (-873 to -156)
	2	706 (568 to 842)	-1035 (-1134 to -949)	-329 (-431 to -220)	36 (22 to 52)	-293 (-377 to -205)
GK *Typha–Hydrocharis*	1	921 (841 to 982)	-771 (-842 to -665)	151 (41 to 300)	60 (47 to 77)	210 (111 to 360)
	2	973 (818 to 1156)	-1086 (-1476 to -862)	-113 (-418 to 66)	68 (52 to 92)	-45 (-343 to 142)
GK *Carex–Lysimachia*	1	1105 (1007 to 1207)	-940 (-1081 to -774)	166 (66 to 252)	86 (63 to 121)	252 (145 to 356)
	2	1270 (1221 to 1362)	-1054 (-1243 to -789)	216 (48 to 470)	85 (59 to 142)	301 (137 to 552)
GK *Phragmites–Lemna*	1	936 (733 to 1200)	-1547 (-1726 to -1386)	-611 (-819 to -450)	100 (48 to 147)	-516 (-747 to -349)
	2	1092 (937 to 1210)	-2267 (-2733 to -1843)	-1175 (-1567 to -690)	101 (61 to 177)	-1074 (-1453 to -565)

Uncertainties on the site level include the uncertainties of the plot models and the spatial heterogeneity. They were calculated by pooling the plot specific annual models derived by error calculation. Different CO_2 balances of the H-Approach and the LS-Approach were accounted for by adding the differences randomly to 50% of the respective annual values derived by error calculation with the H-Approach. To derive uncertainties of C balances the annual models of NEE and CH_4 derived by plot–wise error calculation were summarized and combined site–wise.

Table 3. Small scale spatial variability of net CO_2 and CH_4 emissions

	Absolute small scale spatial variability (g C m^{-2} yr^{-1})[a]		Relative small scale spatial variability (%)[b]	
	NEE	CH_4 emissions	NEE	CH_4 emissions
BA *Eriophorum–Carex*	16 ± 13	0.5 ± 0.2	89 ± 105	4 ± 2
BA *Carex–Equisetum*	9 ± 5	1.4 ± 0.7	19 ± 12	10 ± 5
BA *Phragmites–Carex*	125 ± 140	6.4 ± 2.7	25 ± 25	17 ± 7
GK *Typha–Hydrocharis*	121 ± 66	3.2 ± 3.2	97 ± 63	5 ± 5
GK *Carex–Lysimachia*	95 ± 73	10.9 ± 8.3	47 ± 33	13 ± 10
GK *Phragmites–Lemna*	187 ± 153	24.2 ± 10.0	20 ± 11	25 ± 10

Given are means ± standard deviations, n = 6.
[a] absolute differences between annual plot emissions and annual site emissions.
[b] absolute differences between annual plot emissions and annual site emissions in percentages of absolute values of annual site emissions.

Table 4. GHG balances based on the global warming potentials of CO_2, CH_4 and N_2O for a time horizon of 100 yr (GWP_{100} of CO_2=1, of CH_4=28 and of N_2O=265 CO_2–equivalents, Myhre et al., 2013) with 90% confidence intervals.

Site	Year	CO_2 balance (t CO_2 eq ha^{-1} yr^{-1})	CH_4 balance (t CO_2 eq ha^{-1} yr^{-1})	N_2O balance (t CO_2 eq ha^{-1} yr^{-1})	GHG balance (t CO_2 eq ha^{-1} yr^{-1})
BA *Eriophorum–Carex*	1	-3.1 (-4.8 to -1.4)	3.8 (2.9 to 5.0)	-0.1 (-0.8 to 0.8)	0.5 (-1.4 to 3.1)
	2	-0.3 (-1.8 to 0.8)	4.2 (3.6 to 5.1)	0.2 (-0.2 to 0.8)	4.1 (2.3 to 6.0)
BA *Carex–Equisetum*	1	-3.2 (-3.2 to -2.5)	6.4 (5.0 to 8.0)	-0.1 (-0.7 to 0.5)	3.1 (1.9 to 5.0)
	2	0.9 (-0.2 to 2.1)	4.7 (3.2 to 6.1)	-0.3 (-0.9 to 0.2)	5.3 (3.3 to 7.3)
BA *Phragmites–Carex*	1	-19.4 (-34.2 to -7.1)	15.6 (10.4 to 21.6)	-0.3 (-2.9 to 3.0)	-4.1 (-16.9 to 11.9)
	2	-12.1 (-15.8 to -8.1)	13.3 (8.4 to 19.4)	-0.6 (-3.6 to 2.0)	0.7 (-6.5 to 6.6)
GK *Typha–Hydrocharis*	1	5.5 (1.5 to 11.0)	22.3 (17.4 to 28.6)	0.6 (-1.7 to 2.7)	28.5 (21.5 to 38.9)
	2	-4.2 (-15.3 to 2.4)	25.5 (19.3 to 34.4)	0.4 (-0.7 to 1.5)	21.7 (7.6 to 36.1)
GK *Carex–Lysimachia*	1	6.1 (2.4 to 9.2)	32.3 (23.6 to 45.5)	-0.1 (-2.1 to 1.8)	38.2 (27.8 to 53.7)
	2	7.9 (1.8 to 17.2)	31.6 (22.2 to 53.1)	0.4 (-0.8 to 1.9)	39.9 (25.8 to 60.7)
GK *Phragmites–Lemna*	1	-22.4 (-30.0 to -16.5)	35.7 (18.0 to 54.7)	0.6 (-2.4 to 3.8)	13.9 (-10.6 to 36.0)
	2	-43.1 (-57.5 to -25.3)	37.7 (22.9 to 66.2)	0.0 (-3.5 to 3.4)	-5.4 (-29.2 to 40.0)

Confidence intervals include the uncertainties of the plot models and the spatial heterogeneity. To derive uncertainties of GHG balances the annual models of CO_2 (NEE), CH_4 and N_2O derived by plot–wise error calculation were summarized and combined site–wise.

Table 5. Estimation of net primary production (NPP), heterotrophic (R_h) and autotrophic respiration (R_a) from the *Phragmites australis* sites.

site	year	GPP (g CO_2–C m^{-2} yr^{-1})	NEE (g CO_2–C m^{-2} yr^{-1})	AGB, green (g C m^{-2})[a]	Assumed ratio BG NPP/ AG NPP[b]	NPP (g C m^{-2} yr^{-1})[c]	R_h (g CO_2–C m^{-2} yr^{-1})[d]	R_a (g CO_2–C m^{-2} yr^{-1})[e]	R_a/[GPP]
BA *Phragmites–Carex*	1	-1141	-528	260	1.4	624	96	517	0.45
	2	-1035	-329	169	1.4	406	77	629	0.61
GK *Phragmites–Lemna*	1	-1547	-611	322	1.2	707	96	840	0.54
	2	-2267	-1175	586	1.2	1289	114	978	0.43

[a] Green above ground biomass (AGB) present at end of the first measuring year was estimated for each GHG–plot from biomass harvest at three to four sample plots (40 cm × 40 cm) close to collars accordingly to the share of green vs. dead culms. At the end of the second year green AGB of the plots was calculated from the plot harvest (Table 1) accordingly to the share of green vs. dead culms.

[b] Green AGB was assumed to equal above ground net primary production (AG NPP), although this may underestimate NPP by about 10% (Westlake, 1982). Reported below ground net primary production (BG NPP) to AG NPP ratios range from 0.34 – 2.58 (Westlake, 1982; Scarton et al., 1999; Soetaert et al., 2004; Asaeda et al., 2006). We used the estimate of 1.4 from reeds in North Jutland (Schierup, 1978; cited in Westlake, 1982) for BA *Phragmites–Carex* and a lower ratio (1.2) for GK *Phragmites–Lemna*, because below ground biomass allocation of *Phragmites australis* was found to be proportionally less in deep (70 or 75 cm), compared to shallow (20 or 5 cm) water (Vretare et al., 2001).

[c] net primary production (NPP) = AG NPP plus BG NPP

[d] heterotrophic respiration (R_h) = NPP minus [NEE]

[e] autotrophic respiration (R_a) = [GPP] minus NPP

Table 6. Net annual CO_2 and CH_4 emissions from temperate wetlands with vegetation comparable to Barcianicha' and Giel'čykaŭ Kašyl'.

Location, climate[a]	Site description, method[b]	Dominant plant species	Study years	water level[c] (cm above surface)	NEE[d] (g CO_2–C m^{-2} yr^{-1})	CH_4 emissions[d] (g CH_4–C m^{-2} yr^{-1})	Reference
Oweninny bog, Ireland, 54.12°N 9.58°W (Cfb)	cutover blanket bog with oligotrophic, acid peat, rewetted 2003 (ch)	*Eriophorum angustifolium*	2009 to 11	7±1	-348 ± 222	5.3 ± 0.1	Wilson et al., 2013
Turraun, Ireland, 53.28°N 7.75°W (Cfb)	cutover bog with slightly acidic peat and calcareous subsoil, rewetted 1991 (ch)	*E. angustifolium – Carex rostrata*	2002 to 03	5, -6.3	163, 408	3.2, 2.4	Wilson et al., 2007, 2009
		Typha latifolia	2002 to 03	7, 0.3	266, 451	29.1, 21.6	
Trebel valley mire complex, NE Germany, 54.10°N 12.73°E (Cfb)	former fen grassland, rewetted 1997 (ch)	*Phragmites australis*	2011/12 to 2012/13	-9, -19	-83, 68	11, 1	Günther et al., 2014
		T. latifolia		6, -4	-43, 94	10, 3	
		C. acutiformis		5, -3	-3, 81	47, 3	
Mokre´ Louky, Czech Republic, 49.02°N 14.77°E (Cfb)	eutrophicated sedge fen (ec)	*C. acuta*	2006 to 08	-20 to 10	-199±66		Dušek et al. 2012
Vejlerne Nature Reserve, Denmark, 56.93°N 9.05°E (Cfb)	brackish wetland (ch, 10 occasions, two years)	*P. australis*		summer – to winter +	-552	48	Brix et al., 2001
Horstermeer, Netherlands, 52.14°N 5.04°E (Cfb)	land along the ditches of a former fen grassland, rewetted about 1995 (ch)	*P. australis – T. latifolia*	2006	-2 to 5		87.6	Hendriks et al., 2007
Newport News Swamp, Virginia, USA, 37°N 76.5°W (Cfb)	freshwater marsh, 20 cm organic layer (ch)	*T. latifolia*	1992/93	5 to 20	-896	81.6	Whiting and Chanton, 2001
Florida, USA, 30.5°N 84.25°W (Cfa)	lake shore (ch)	*T. latifolia*	1992 to 93	5 to 20	-978, -1139	51.6, 72.0	
San Joaquin Freshwater Marsh, California, USA, 33.66°N 117.85°W (Csb)	freshwater marsh (ec)	*T. latifolia*	1999 to 03	summer – to winter +	136±363		Rocha and Goulden, 2008
Sacramento–San Joaquin Delta, California, USA, 1st site: 38.05°N 121.77°W, 2nd site: 38.11°N 121.65°W (Csa)	former fen pasture, rewetted 2010 (ec)	*T. spp., Schoenoplectus acutus*	2012/13	107	-368	53	Knox et al., 2015
	former agricultural fen, rewetted 1997 (ec)			26	-397	38.7	
Mer Bleue, Ontario, Canada, 45.4°N 75.5°W (Dfb)	freshwater marsh (ec – NEE, ch – CH_4)	*T. angustifolia*	2005 to 09	at surface	−224 ± 54	127 ± 19	Strachan et al., 2015
Ballards Marsh, Nebraska, USA, 42.87°N 100.55°W (Dfa)	freshwater marsh, 10 to 30 cm litter (ec)	*P. australis*	1994	40 to 60		60	Kim et al., 1998
Winous Point, Lake Erie, Ohio, USA, 41.47°N 83°W (Dfa)	freshwater marsh, 20 cm organic layer (ec)	*T. angustifolia – Nymphaea odorata*	2011 to 13	20 to 60	65±92	50.8 ± 6.9	Chu et al., 2015
Lake Vesijärvi, S Finland, 61.08°N 25.50°E (Dfc)	inundated peatland on the shore of an eutrophic lake (ch)	*P. australis*	1997 to 99	10 to 20		33 ± 13.5	Kankaala et al., 2004
		P. australis	1997 to 99	30 to 70		122.3 ± 56.5	
Loch Vale watershed, Colorado, USA, 40.29°N 105.66°W (Dfc)	pristine sedge fen (ch)	*C. aquatilis*	1996 to 98	water saturated	81±4	31.2 ± 2.1	Wickland et al., 2001
Panjin Wetland, Liaoning Province, NE China, 41.13°N 121.90°E (Dwa)	freshwater tidal wetland with silty clay (ec)	*P. australis*	2005	vol. SWC 3% to 46%	-65		Zhou et al., 2009

[a] climate type after Köppen and Geiger (Kottek et al., 2006): Cfb – Warm temperate, fully humid, warm summer; Cfa – Warm temperate, fully humid, hot summer; Csb – Warm temperate with dry and warm summer; Csa – Warm temperate with dry and hot summer; Dfb – Snow climate, fully humid, warm summer; Dfa – Snow climate, fully humid, hot summer; Dfc – Snow climate, fully humid, cool summer and cold winter; Dwa – Snow climate with dry winter and hot summer

[b] ch – chamber method, ec – eddy covariance method

[c] annual water level (listed for one or two years, but given as mean ± standard deviation when three or more years) or water level range (water level of dry to water level of wet season)

[d] annual NEE and methane emissions, listed for one or two years, but given as mean ± standard deviation when three or more years

Table A1. Plant species cover of GHG measuring plots in summer 2010 and 2012.

	BA						BA						BA					
	Eriophorum–Carex						***Carex–Equisetum***						***Phragmites–Carex***					
	2010			2012			2010			2012			2010			2012		
species	I	II	III	I	II	III	I	II	III	I	II	III	I	II	III	I	II	III
Eriophorum angustifolium	6	6	7	6	6	6												
Marchantia polymorpha	3	2	2						2									
Dicranella cerviculata	3	2	2	3	4	4		6	2									
Juncus cf. *compressus*		1		3	2	2	2	2		2	2	2						
Utricularia intermedia											2	2	7	6	7			
Chara spec.										2		3				1		
green algae												4				2		
Phragmites australis											1		7	8	6	8	8	8
Dicranella heteromalla													2	2	2			
Carex rostrata	2	2	3	2	2	2	7	7	6	7	6	6	3	3	3	3	3	3
Equisetum fluviatile	2			2	2		2	2	2	2	2	2	1	1	1	1		1
Salix cinerea	1	1		1			1	1	1	1			1		4	1		
Drepanocladus aduncus			2										5			2		4

	GK						GK						GK					
	Carex–Lysimachia						***Typha–Hydrocharis***						***Phragmites–Lemna***					
	2010			2012			2010			2012			2010			2012		
species	I	II	III	I	II	III	I	II	III	I	II	III	I	II	III	I	II	III
Thelypteris palustris	4					6												
Calamagrostis neglecta	4					2												
Carex elata	2	5	6	8	5	2			7			8						
Carex vesicaria	7	2		3	6	2	2	3		5	5							
Typha latifolia	6	7	6		4	4	6	7	3	6	3	4						
Galium palustre	2	2	2	2	2	2				2	2	2						
Cardamine amara	2	2	1	2	2				1	2	1	2						
Lycopus europeus		2		2	2	2			1		1	1						
Lysimachia thyrsiflora	1	2	2	3	2	2				2	4	2						
Lemna trisulca							2				2			1		2	2	2
Phragmites australis													7	7	8	9	7	8
Stratiotes aloides													1	6			5	2
Drepanocladus aduncus	2	5	2	6	8	3	3	2	2	8	3	7	2			2		2
Hydrocharis morsus–ranae				2	3	2	3	3	2	4	6	3	3	5	4	5	8	6
Lemna minor					2	2	2	1		2	2	2	1	1		2		

Vegetation types of sites studied in Barcianicha: *Eriophorum angustifolium–Carex rostrata*–reed (BA *Eriophorum–Carex*), *Carex rostrata–Equisetum fluviatile*–reed (BA *Carex–Equisetum*), *Phragmites australis–Carex rostrata*–reed (BA *Phragmites–Carex*), and Giel'čykaŭ Kašyl': *Carex elata–Lysimachia thyrsiflora*–reed (GK *Carex–Lysimachia*), *Typha latifolia–Hydrocharis morsus–ranae*–reed (GK *Typha–Hydrocharis*), *Phragmites australis–Lemna trisulca*–reed (GK *Phragmites–Lemna*). Plant cover scale according to Peet et al. (1998): Class 1 = very few individuals, 2 = cover of 0–1%, 3 = 1–2%, 4 = 2–5%, 5 = 5–10%, 6 = 10–25%, 7 = 25–50%, 8 = 50–75%, 9 = 75–95%, 10 >=95%. Species not exceeding cover class 2 are only shown if they meet class 2 in more than two relevés.

Table A2.

Mean ± Std. Error of daytime (PAR > 2 µmol m^{-2} s^{-1}) CH_4 flux rates, PAR, T_{in}, and RH_{in} by plot and chamber type (DF = opaque mixed chamber, TF = transparent mixed chamber, D = not mixed opaque chamber). Values with same letter superscript do not differ significantly at $P < 0.05$ (Mann-Whitney or Kruskal-Wallis test; *post-hoc* non-parametric Nemenyi test), data of *BA Phragmites-Carex II* and *GK Phragmites-Lemna II* from Minke et al. (2014).

Site, plot and date	Chamber type	N	PAR (µmol m^{-2} s^{-1})	T_{in} (°C)	dT_{in} (°C)	RH_{in} (%)	dRH_{in} (%)	CH_4 flux (mg CH_4-C m^{-2} h^{-1})	Methane factor
BA Eriophorum-Carex I	DF	8	685^{a} ± 208	16.6^{a} ± 1.1	1.0^{a} ± 0.2	90.2^{a} ± 2.6	7.5^{a} ± 1.7	2.30^{a} ± 0.10	TF/DF = 1.09
2012-07-18	TF	7	1145^{a} ± 224	17.1^{a} ± 1.5	3.0^{b} ± 0.5	78.6^{a} ± 4.1	3.8^{a} ± 0.8	2.49^{a} ± 0.05	
BA Carex-Equisetum III	DF	7	937^{a} ± 401	17.4^{a} ± 1.4	1.5^{a} ± 0.4	90.1^{a} ± 2.1	5.8^{a} ± 1.7	2.30^{a} ± 0.08	TF/DF = 0.99
2012-07-18	TF	6	851^{a} ± 164	17.8^{a} ± 1.5	1.5^{a} ± 0.3	80.2^{b} ± 3.0	4.2^{a} ± 1.3	2.28^{a} ± 0.08	
BA Carex-Equisetum III	D	14	482^{a} ± 85	15.4^{a} ± 0.7	0.7^{ab}± 0.1	79.4^{ab} ± 2.6	9.1^{a} ± 1.0	0.76^{a} ± 0.03	TF/D = 1.07
2012-09-16	DF	14	535^{a} ± 95	15.6^{a} ± 0.7	0.5^{a} ± 0.1	86.2^{a} ± 1.5	7.5^{ab} ± 0.8	0.80^{a} ± 0.04	TF/DF = 1.02
	TF	13	584^{a} ± 95	15.3^{a} ± 0.6	1.3^{b}± 0.2	75.4^{b} ± 2.3	4.4^{b} ± 0.6	0.81^{a} ± 0.02	
GK Typha-Hydrocharis I	DF	9	869^{a} ± 157	24.3^{a} ± 1.2	1.0^{a} ± 0.2	94.4^{a} ± 1.7	18.1^{a} ± 3.7	16.61^{a} ± 0.43	TF/DF = 1.18
2012-07-12	TF	9	868^{a} ± 149	24.9^{a} ± 0.9	1.4^{a} ± 0.3	88.6^{a} ± 2.7	14.8^{a} ± 2.3	19.52^{b} ± 1.20	
GK Typha-Hydrocharis I	DF	11	821^{a} ± 136	19.9^{a} ± 1.2	0.8^{a} ± 0.2	85.3^{a} ± 3.0	15.5^{a} ± 2.8	14.04^{a} ± 0.24	TF/DF = 1.20
2012-07-13	TF	10	1097^{a} ± 146	20.7^{a} ± 1.4	1.7^{b} ± 0.3	80.3^{a} ± 3.7	11.8^{a} ± 2.1	18.00^{b} ± 0.20	
GK Carex-Lysimachia I	DF	9	923^{a} ± 115	24.2^{a} ± 1.1	1.0^{a} ± 0.2	84.9^{a} ± 3.0	9.2^{a} ± 1.5	14.28^{a} ± 0.22	TF/DF = 1.10
2012-07-12	TF	9	749^{a} ± 111	24.8^{a} ± 1.1	1.5^{a} ± 0.3	82.3^{a} ± 2.9	7.0^{a} ± 1.4	15.76^{b} ± 0.38	
GK Carex-Lysimachia I	DF	11	1207^{a} ± 188	20.1^{a} ± 1.3	1.4^{a} ± 0.2	83.4^{a} ± 3.3	12.7^{a} ± 2.1	14.62^{a} ± 0.33	TF/DF = 1.08
2012-07-13	TF	10	1121^{a} ± 177	21.1^{a} ± 1.5	3.0^{b} ± 0.5	78.8^{a} ± 4.3	7.5^{a} ± 1.2	15.81^{b} ± 0.23	
BA Phragmites-Carex II	D	16	830^{a} ± 130	19.4^{a} ± 1.1	0.6^{a} ± 0.2	81.0^{a} ± 3.2	11.8^{ab} ± 1.8	9.86^{a} ± 1.40	TF/D = 1.01
2012-08-08	DF	16	857^{a} ± 133	19.7^{a} ± 1.1	0.9^{a} ± 0.2	81.9^{a} ± 3.3	13.4^{a} ± 2.2	10.17^{a} ± 1.50	TF/DF = 0.98
	TF	16	735^{a} ± 121	19.2^{a} ± 1.2	0.8^{a} ± 0.1	76.5^{a} ± 3.7	6.0^{b} ± 1.0	9.95^{a} ± 1.51	
GK Phragmites-Lemna II	D	14	707^{a} ± 130	20.6^{a} ± 1.2	0.7^{ab} ± 0.2	70.4^{a} ± 3.2	6.0^{a} ± 1.5	13.70^{a} ± 1.68	TF/D = 1.27
2011-09-21	DF	13	819^{a} ± 125	21.7^{a} ± 1.3	1.0^{a} ± 0.2	71.1^{a} ± 3.1	13.8^{b} ± 1.8	17.42^{a} ± 2.39	TF/DF = 1.00
	TF	12	893^{a} ± 125	23.1^{a} ± 1.0	1.8^{b} ± 0.2	66.5^{a} ±2.5	6.6^{a} ± 1.0	17.46^{a} ± 2.08	

Table A3. Annual fluxes of CO_2, CH_4, and N_2O with confidence intervals

site	year	plot	R_{eco} (g CO_2-C m^{-2} yr^{-1})	GPP (g CO_2-C m^{-2} yr^{-1})	NEE (g CO_2-C m^{-2} yr^{-1})	CH_4 emissions (g CH_4-C m^{-2} yr^{-1})	N_2O emissions (mg N_2O -N m^{-2} yr^{-1})
BA *Eriophorum-Carex*	1th	I	378 (359 to 398)	-496 (-514 to -478)	-118 (-132 to -104)	11 (9 to 14)	-80 (-189 to 21)
		II	358 (338 to 378)	-441 (-449 to -433)	-83 (-102 to -63)	10 (8 to 12)	-89 (-213 to 49)
		III	355 (338 to 372)	-411 (-415 to -406)	-56 (-75 to -37)	10 (8 to 13)	79 (-65 to 245)
	2nd	I	436 (413 to 459)	-444 (-451 to -437)	-8 (-35 to 19)	12 (10 to 14)	32 (-67 to 130)
		II	391 (367 to 414)	-413 (-421 to -406)	-23 (-51 to 6)	11 (9 to 12)	39 (-38 to 115)
		III	390 (379 to 401)	-381 (-387 to -375)	9 (-5 to 23)	11 (10 to 14)	95 (-75 to 284)
BA *Carex-Equisetum*	1th	I	210 (195 to 226)	-287 (-296 to -278)	-77 (-87 to -66)	15 (13 to 18)	-40 (-148 to 71)
		II	245 (227 to 263)	-350 (-362 to -338)	-105 (-115 to -95)	19 (16 to 23)	-21 (-132 to 85)
		III	241 (226 to 255)	-322 (-334 to -310)	-82 (-88 to -76)	17 (14 to 21)	-23 (-203 to 168)
	2nd	I	303 (280 to 326)	-286 (-292 to -280)	17 (-9 to 43)	10 (8 to 13)	-28 (-110 to 56)
		II	353 (334 to 372)	-331 (-335 to -327)	22 (2 to 43)	14 (13 to 19)	-84 (-150 to -12)
		III	323 (300 to 347)	-290 (-295 to -284)	34 (10 to 57)	14 (12 to 16)	-113 (-296 to 79)
BA *Phragmites-Carex*	1th	I	498 (473 to 522)	-967 (-999 to -935)	-469 (-517 to -421)	32 (26 to 39)	-515 (-833 to -226)
		II	693 (646 to 741)	-1555 (-1600 to -1509)	-861 (-942 to -780)	46 (34 to 57)	356 (-246 to -982)
		III	650 (594 to 705)	-902 (-921 to -884)	-253 (-318 to -188)	48 (36 to 61)	-75 (-487 to 335)
	2nd	I	615 (562 to 669)	-963 (-980 to -947)	-348 (-410 to -285)	30 (21 to 35)	-63 (-977 to 849)
		II	769 (691 to 848)	-1122 (-1136 to -1108)	-353 (-437 to -269)	45 (36 to 57)	-466 (-943 to 849)
		III	732 (680 to 785)	-1018 (-1052 to -984)	-286 (-360 to -212)	32 (24 to 42)	87 (-174 to 374)
GK *Typha-Hydrocharis*	1th	I	877 (836 to 918)	-801 (-813 to -790)	76 (36 to 116)	59 (49 to 73)	95 (-673 to 886)
		II	923 (912 to 934)	-831 (-844 to -817)	92 (74 to 111)	59 (47 to 73)	130 (-279 to 533)
		III	963 (942 to 984)	-680 (-697 to -663)	284 (263 to 304)	61 (44 to 83)	220 (-52 to 515)
	2nd	I	1104 (1046 to 1161)	-1446 (-1480 to -1412)	-342 (-424 to -261)	63 (51 to 75)	151 (-124 to 449)
		II	827 (816 to 838)	-870 (-881 to -859)	-43 (-60 to -27)	65 (50 to 82)	74 (-223 to 372)
		III	988 (972 to 1005)	-943 (-967 to -919)	46 (20 to 72)	77 (59 to 103)	76 (-111 to 257)
GK *Carex-Lysimachia*	1th	I	1124 (1090 to 1158)	-962 (-989 to -934)	162 (135 to 189)	86 (74 to 100)	-137 (-677 to 419)
		II	1167 (1124 to 1211)	-1065 (-1084 to -1047)	102 (60 to 144)	72 (59 to 86)	162 (-160 to 505)
		III	1024 (1005 to 1044)	-792 (-814 to -770)	233 (206 to 259)	101 (75 to 140)	-91 (-358 to 160)
	2nd	I	1246 (1224 to 1268)	-811 (-837 to -785)	435 (395 to 475)	84 (65 to 121)	100 (-140 to 346)
		II	1331 (1296 to 1367)	-1205 (-1248 to -1162)	126 (56 to 196)	67 (56 to 82)	-56 (-220 to 88)
		III	1233 (1219 to 1246)	-1146 (-1188 to -1104)	87 (42 to 132)	102 (76 to 162)	229 (-128 to 599)
GK *Phragmites-Lemna*	1th	I	921 (892 to 949)	-1446 (-1511 to -1380)	-525 (-607 to -443)	113 (88 to 139)	58 (-524 to 684)
		II	767 (729 to 804)	-1516 (-1568 to -1465)	-750 (-827 to -673)	61 (43 to 83)	-101 (-783 to 548)
		III	1121 (1037 to 1206)	-1680 (-1737 to -1623)	-559 (-623 to -495)	112 (73 to 164)	468 (-256 to 1176)
	2nd	I	1170 (1122 to 1219)	-2678 (-2745 to -2611)	-1507 (-1584 to -1431)	87 (65 to 113)	99 (-652 to 872)
		II	970 (929 to 1012)	-2235 (-2362 to -2108)	-1265 (-1381 to -1149)	77 (57 to 110)	-437 (-1017 to 140)
		III	1135 (1062 to 1208)	-1887 (-1939 to -1836)	-752 (-825 to -679)	139 (86 to 202)	330 (-253 to 937)

Uncertainties of CO_2 balances on the plot level were calculated as 50% of the difference between the H-Approach and the LS-Approach plus the 90% CI's of the H-Approach. Plot level uncertainties for CH_4 represent the 90% confidence intervals (CI's) of the models, but for N_2O only the 90% CI's of the measured N_2O fluxes.

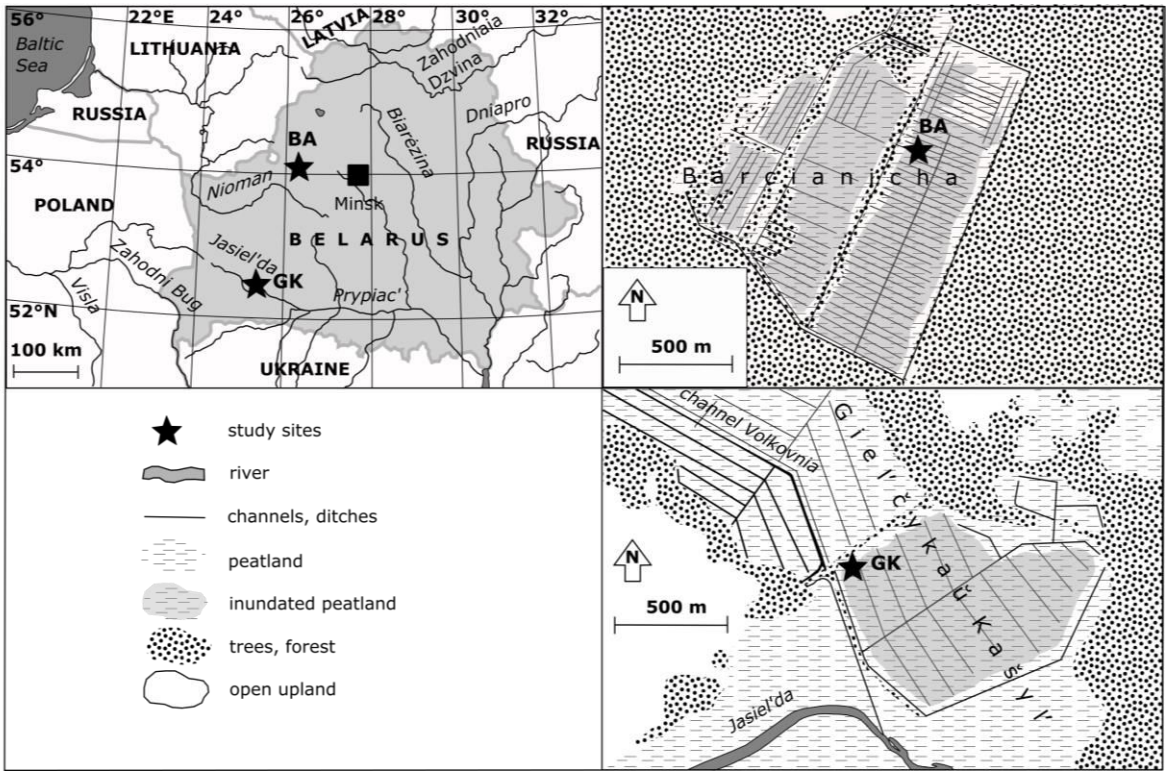

Figure 1. Location of the study sites

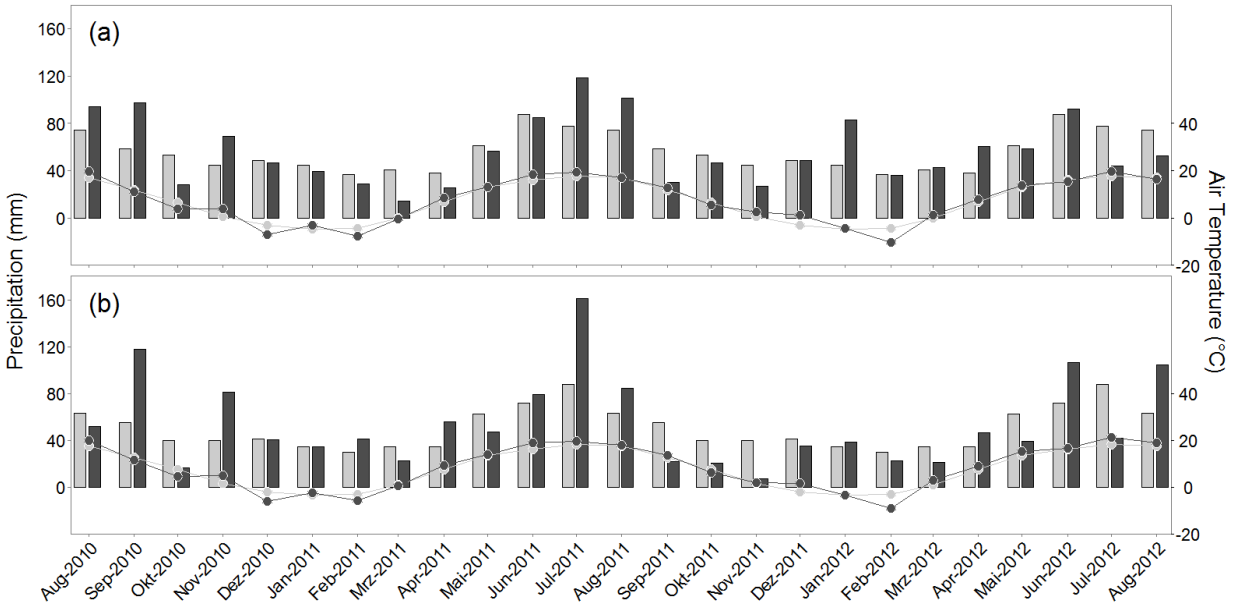

Figure 2. Cumulative monthly precipitation (bars) and average monthly air temperatures (dots) for Barcianicha (A) and Giel'čykaŭ Kašyl' (B). Actual temperatures (black) were measured in (A) Višnieva, 5.6 km NW of Barcianicha, and (B) Z'dzitava, 6.3 km NE of Giel'čykaŭ Kašyl'. Actual precipitation data (black) and 30 year averages (1979–2008) of temperatures and precipitation (grey) are from meteorological stations of "Gidrometcentr" in (A) Valožyn, 15 km E of Barcianicha, and (B) Pružany, 54 km WNW of Giel'čykaŭ Kašyl'.

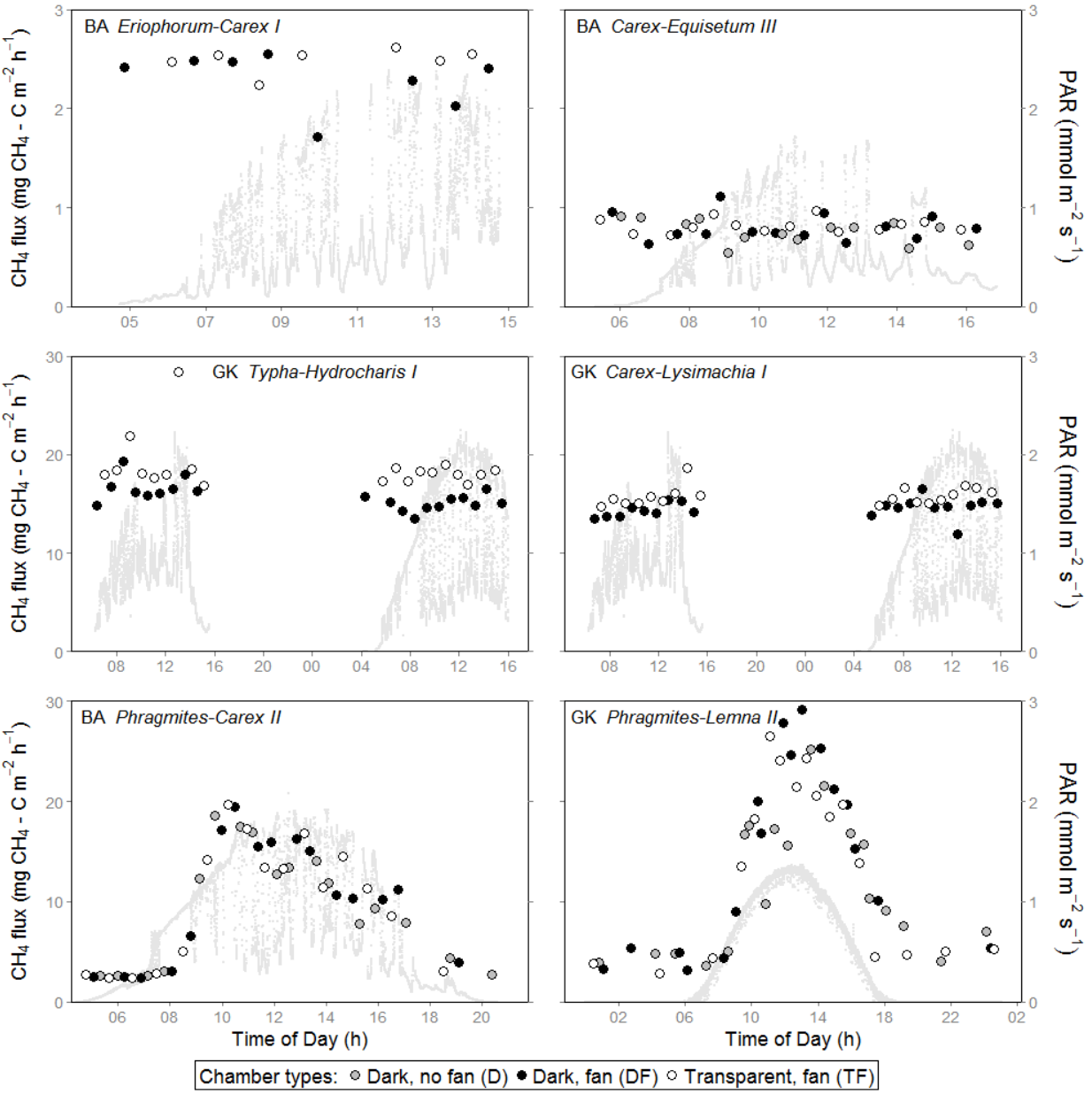

Figure 3. Diurnal variation of methane emissions, measured with different chamber types, and outside PAR, at BA *Eriophorum–Carex* (plot I, 18 July 2012), BA *Carex–Equisetum* (plot III, 16 September 2012), BA *Phragmites–Carex* (plot II, 8 August 2012), GK *Typha–Hydrocharis* and GK *Carex–Lysimachia* (both plot I, 12 Jul 2012 and 13 July 2012), and GK *Phragmites–Lemna* (plot II, 21 September 2011). Data of BA *Phragmites–Carex* and GK *Phragmites–Lemna* are from Minke et al. (2014).

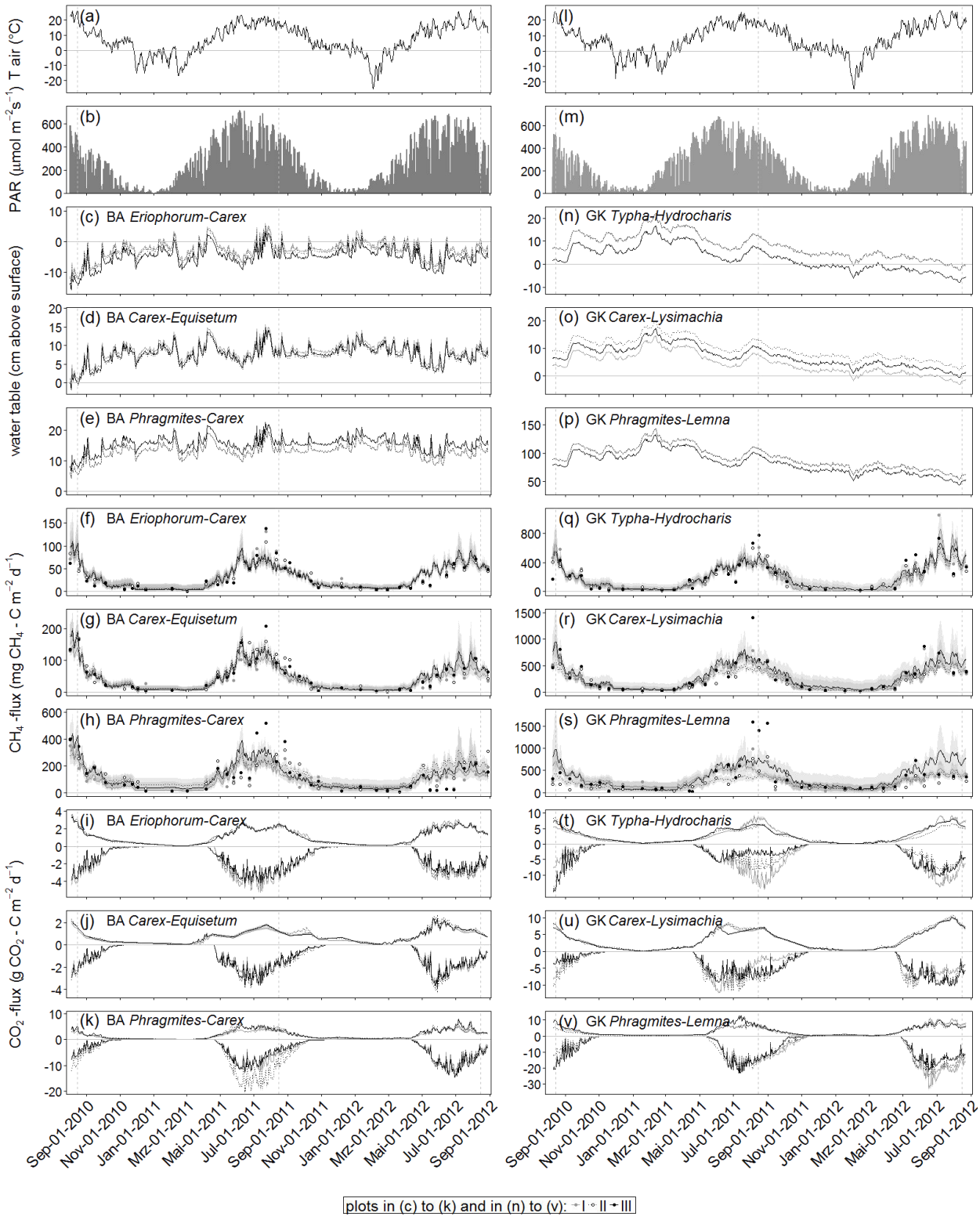

Figure 4. Mean daily air temperature (a) and mean daily PAR (b) at Višnieva (a, b) and Z'dzitava (l, m), mean daily water table positions, mean daily measured (points) and modeled (lines) CH_4 fluxes, and mean daily modeled (H-approach) GPP, and R_{eco} (I, J, K) of Barcianicha (c to k) and Giel'čykaŭ Kašyl' sites (n to v).

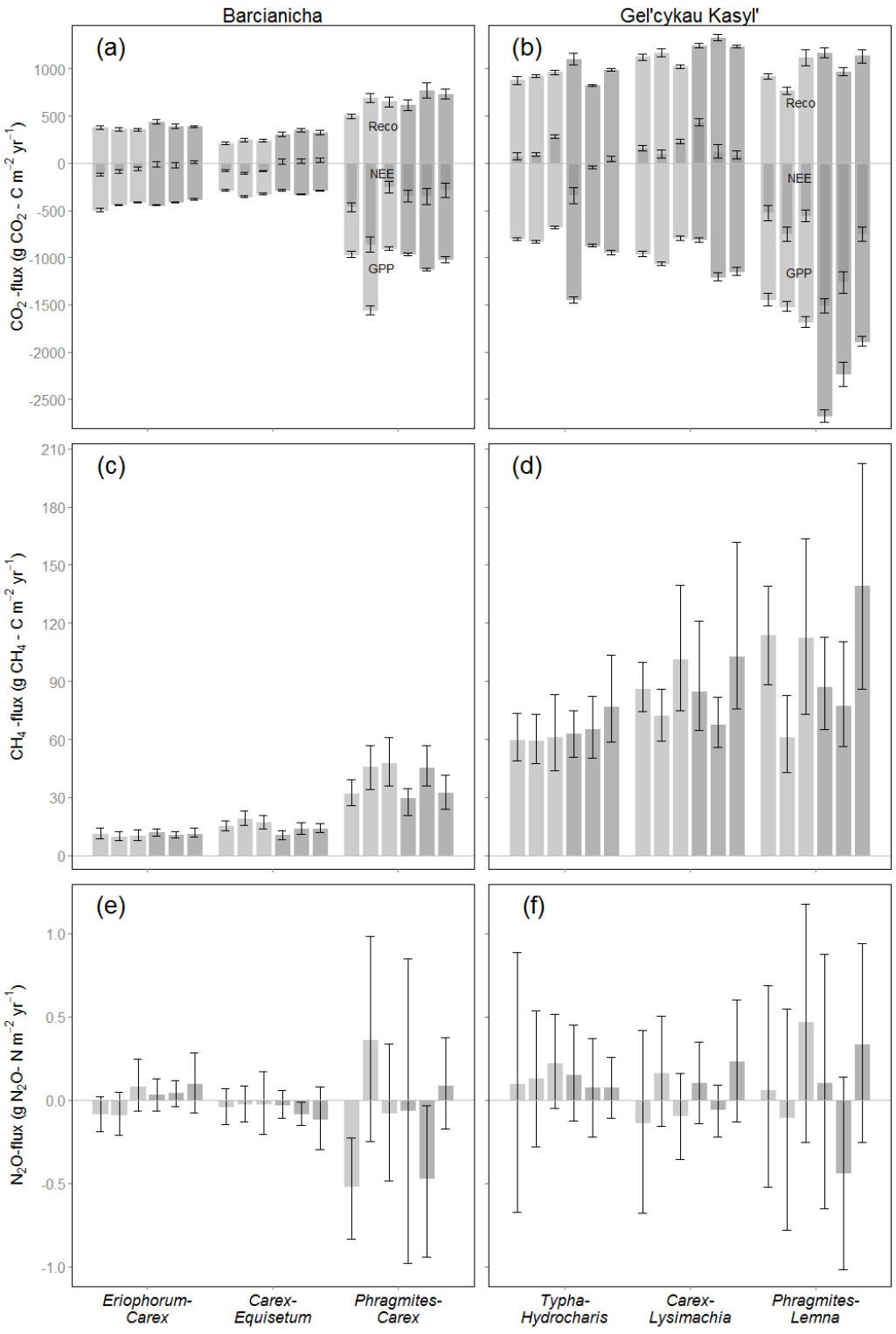

Figure 5. Annual CO_2 (NEE, R_{eco}, GPP), CH_4 and N_2O fluxes at Barcianicha (a, c, e) and Giel'čykaŭ Kašyl' (b, d, f). Uncertainties for CO_2 fluxes are 50% of the difference between both modelling approaches plus the 90 % confidence intervals of the H-approach. Uncertainties for CH_4 represent 90 % confidence intervals of the models, but for N_2O only 90 % CI of the measured N_2O fluxes. Light grey = 1st year, darker grey = 2nd year. Plots are ordered I, II, III.

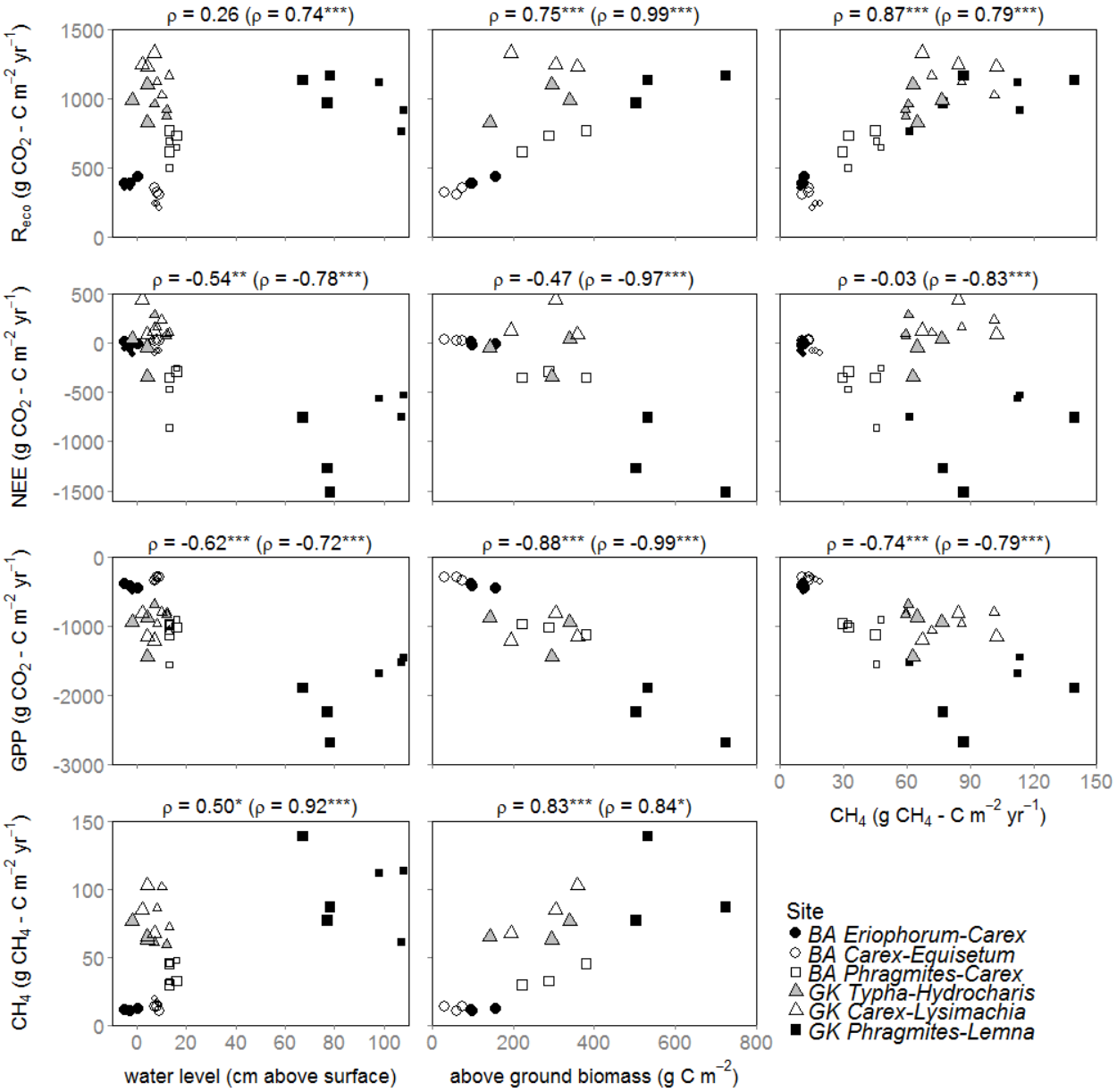

Figure 6. Scatter plots of annual NEE, R_{eco}, GPP, CH_4 emissions, median annual water levels (both years for all plots, n = 36), and above ground biomass carbon (second year for all plots, *n* = 18). Spearman's *ρ* significant at ' $P \leq 0.05$; * $P \leq 0.01$; ** $P \leq 0.001$; *** $P \leq 0.0001$. Spearman's *ρ* in brackets without GK *Typha–Hydrocharis* and GK *Carex–Lysimachia* (*n* = 30 for correlations among water levels and fluxes; *n* = 15 for correlations among biomass and fluxes). Small symbols indicate first year, large symbols second year.